



Grado en Ingeniería en Tecnologías Industriales

Trabajo de Fin de Grado

Characterization of HTS Coils

Autor: Celia Gómez Limia

Director: Loïc Quéval

Madrid
Junio 2022

Declaro, bajo mi responsabilidad, que el Proyecto presentado con el título

CHARACTERIZATION OF HTS COILS

en la ETS de Ingeniería - ICAI de la Universidad Pontificia Comillas en el

curso académico 2021/22 es de mi autoría, original e inédito y

no ha sido presentado con anterioridad a otros efectos.

El Proyecto no es plagio de otro, ni total ni parcialmente y la información que ha sido

tomada de otros documentos está debidamente referenciada.

Fdo.: Celia Gómez Limia

Fecha: 22/ 06/ 2022



Autorizada la entrega del proyecto

EL DIRECTOR DEL PROYECTO

Fdo.: Dr. Loïc Quéval

Fecha: 22/ 06/ 2022



Caracterización de bobinas HTS - Resumen del proyecto

Autor: Gómez Limia, Celia

Supervisor: Quéval, Loïc

Entidad colaboradora: Université Paris-Saclay, GeePs

Resumen

El objetivo principal de este proyecto es contribuir a la normalización de la medición de la característica corriente-voltaje (IV) de las bobinas superconductoras. Para ello, se han realizado varios experimentos con cintas y bobinas superconductoras. Se propone una nueva forma de realizar la caracterización de las bobinas HTS, sin soldar las tomas de potencial en el material superconductor. Su precisión se verifica comparando la característica IV obtenida por el método propuesto con la obtenida mediante el método convencional. El análisis se completa con una simulación por elementos finitos del conector.

Introducción

En el contexto actual de crecimiento continuo de la demanda de electricidad, nos interesa que el transporte de electricidad sea lo más eficiente posible. Somos testigos de las pérdidas Joule en las líneas de transmisión eléctrica convencionales, ya que están compuestas por conductores resistivos. En estas circunstancias, el desarrollo de la superconductividad en el sector de la energía resulta interesante.

Entre otras propiedades, un superconductor tiene resistividad cero cuando se enfría por debajo de su temperatura crítica. Por lo tanto, un cable de alimentación superconductor puede transportar altas corrientes con pérdidas insignificantes.

Entre otros dispositivos superconductores que se han propuesto, el "filtro de potencia superconductor" pretende aumentar la estabilidad de las redes de corriente continua

añadiendo una resistencia dependiente de la corriente a la línea eléctrica. Este filtro se construye utilizando una bobina HTS no inductiva. Para poder utilizar este dispositivo, es necesario caracterizarlo. El primer paso es caracterizar la bobina HTS, ya que no existe ninguna norma para medir esta característica, lo que constituye el objetivo de este proyecto.

Descripción de la propuesta

Un dispositivo HTS se caracteriza por su característica corriente-tensión (IV), es decir, el gráfico que representa la tensión en estado estacionario del dispositivo en función de su corriente. Las característica IV típica de un dispositivo HTS se ilustra en la Figura 1.

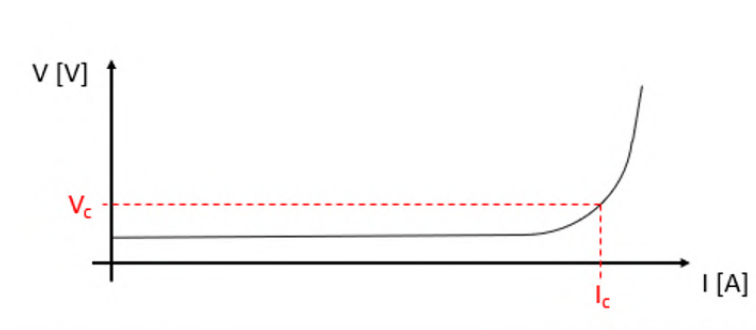


Figura 1: Característica típica de corriente-tensión de un dispositivo HTS

Según la ley de Ohm ($V = RI$), la resistencia corresponde a la pendiente de la característica IV.

La caracterización de una muestra corta de cinta HTS está normalizada. La norma sugiere que la característica IV se mida por el método de las cuatro sondas. Su esquema se muestra en la Figura 2.

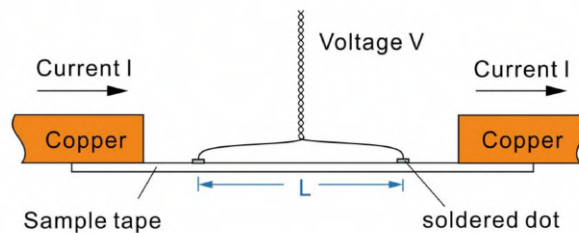


Figura 2: Esquema del método de las cuatro sondas

La corriente es suministrada por una fuente de corriente a dos conectores de cobre en contacto directo con la cinta. Se sueldan dos tomas de potencial en la cinta a 10 cm de distancia para medir la tensión entre ellas con un nanovoltímetro a medida que se aumenta la corriente en pequeños pasos. La curva obtenida es la característica IV de la cinta HTS.

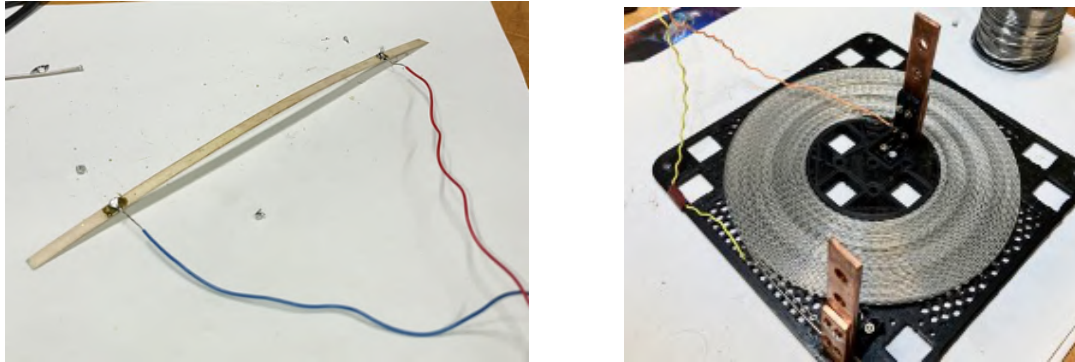


Figura 3: Cinta HTS y bobina HTS

Las cintas HTS se enrollan en bobinas HTS para ser utilizadas en dispositivos HTS, Fig. 3. Al adaptar la norma a las bobinas HTS, se dan numerosos problemas al soldar las tomas de potencial en la bobina. Por lo tanto, se propone una nueva metodología: medir la diferencia de potencial directamente desde los conectores de cobre del soporte, como se muestra en la Figura 4.

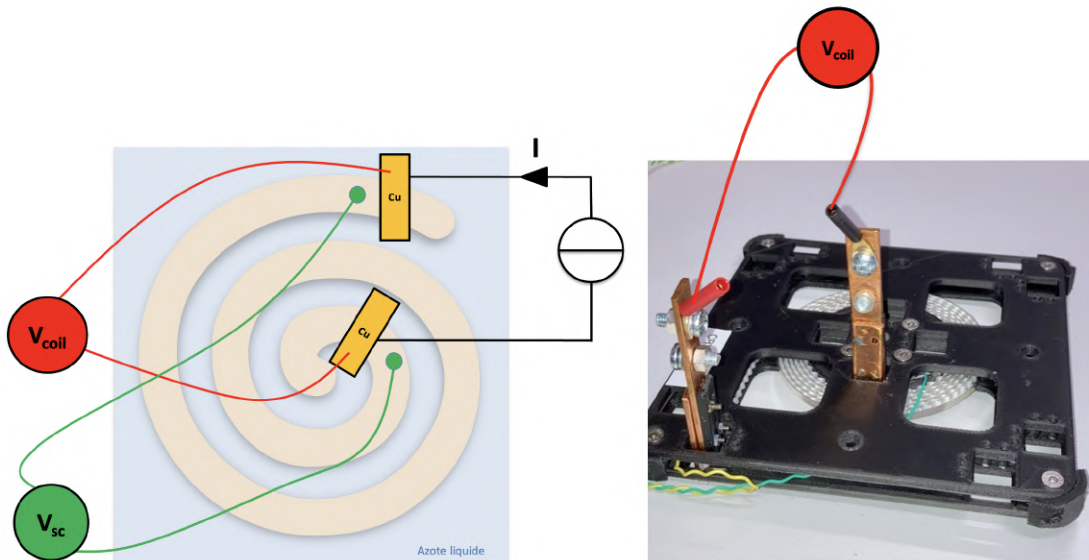


Figura 4: Protocolo de medición propuesto

Nuestros esfuerzos se centran en el cálculo de la resistencia adicional que aparece en la característica IV medida, para eliminarla con el fin de obtener la característica IV real de la bobina HTS.

Medimos tanto V_{coil} como V_{sc} en la bobina para compararlos y sacar conclusiones sobre la naturaleza de la resistencia de los conectores. Llamamos V_{conn} a la diferencia de tensión en cada conector de cobre, obteniendo la siguiente ecuación:

$$V_{sc} = V_{coil} - 2 \cdot V_{conn} \quad (1)$$

donde $V_{conn} = R_{conn} \cdot I$ y R_{conn} es la resistencia de un solo conector de cobre. Al identificar R_{conn} , podremos estimar V_{sc} a partir de V_{coil} .

Results

En las figuras 5 y 6, podemos ver la característica IV de cada bobina medida con los dos métodos.

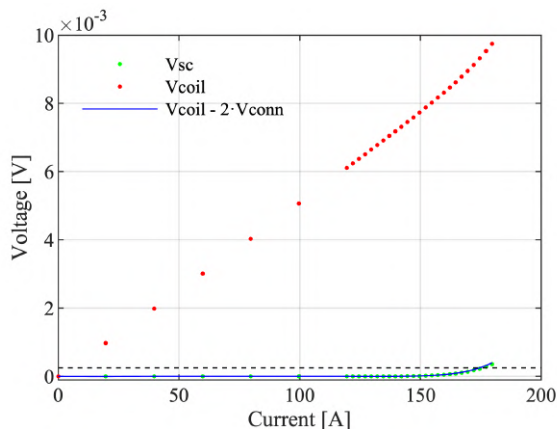


Figura 5: Medida en la bobina inductiva de 2,5 m y ajuste de segundo orden

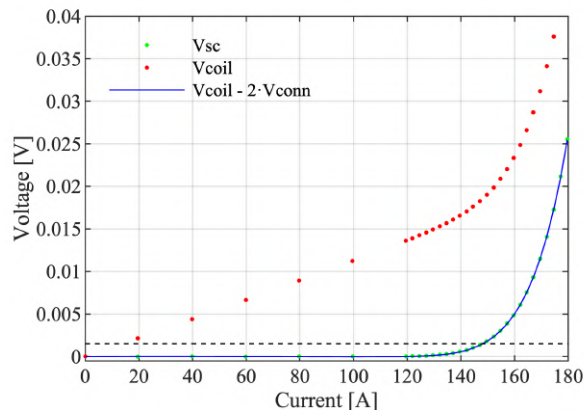


Figura 6: Medida en la bobina inductiva de 15m y ajuste de segundo orden

Para identificar la tensión del conector, se realiza un post-processing asumiendo que la tensión del conector es de segundo orden.

$$V_{conn} = R_c I + R_d I^2 \quad (2)$$

Los resultados del post-processing mostrados en las Figuras 5 y 6 muestran que podemos estimar el voltaje del superconductor V_{sc} a partir de la medida V_{coil} .

Para analizar la hipótesis sobre el orden de tensión del conector, realizamos una simulación termoelectrica por elementos finitos en 3D del conector. Cuando se comparan los resultados obtenidos para V_{conn} por la simulación con los obtenidos experimentalmente, se aprecia una clara diferencia. Esto indica que hay que seguir mejorando el modelo numérico. Para intentar comprender la causa de esta discrepancia, realizamos un análisis de sensibilidad. Esta simulación numérica nos permitió confirmar que la resistencia es, de hecho, una función no constante de la corriente.

Conclusiones

Mediante el post-processing de las medidas realizadas en el laboratorio y la realización de una simulación numérica del conector de cobre, pudimos determinar que su resistencia no es constante. Esta resistencia se aproxima mejor como una función lineal de la corriente, que corresponde a una caída de tensión de segundo orden. Ahora podemos eliminar el efecto de los conectores de la característica IV.

La técnica de medición propuesta es, desde nuestro punto de vista, una mejora de la técnica convencional, ya que elimina la dificultad de soldar las tomas de potencial en el material HTS. Una técnica de caracterización sencilla es interesante para acelerar la adopción de dispositivos HTS.

Characterization of HTS Coils - Project Summary

Author: Gómez Limia, Celia

Supervisor: Quéval, Loïc

Collaborating Entity: Université Paris-Saclay, GeePs

Abstract

The main purpose of this project is to contribute to the standardization of the measurement of the current-voltage (IV) characteristic of superconducting coils. To this end, several experiments have been performed with superconducting tapes and coils. A new way to perform the characterization of HTS coils, without welding potential taps on the superconducting material, is proposed. Its accuracy is verified by comparing the obtained IV characteristic with the one obtained using the conventional method. The discussion is completed with a finite element simulation of the connector.

Introduction

In the current context of the continuous growth of electricity demand, we are interested in making electricity transmission as efficient as possible. We witness Joule losses in conventional power transmission lines, as they are composed of resistive conductors. Under these circumstances, the development of superconductivity in the power sector is of interest.

Among other properties, a superconductor has zero resistivity when cooled down below its critical temperature. A superconducting power cable can therefore carry high currents with negligible losses.

Among others superconducting devices that have been proposed, the "superconducting power filter" aims to increase the stability of DC grids by adding a current dependent resistance to the power line. Such a filter is built using a non-inductive HTS coil. To

be able to use such device, we need to characterize it. The first step is to characterize the HTS coil, as there is no standard to measure this characteristic, this is the focus of this project.

Description of the proposal

An HTS device is characterized by its current-voltage (IV) characteristic, i.e. the graph representing the steady-state voltage of the device as a function its current. The typical IV characteristics of an HTS device is illustrated in Figure 1.

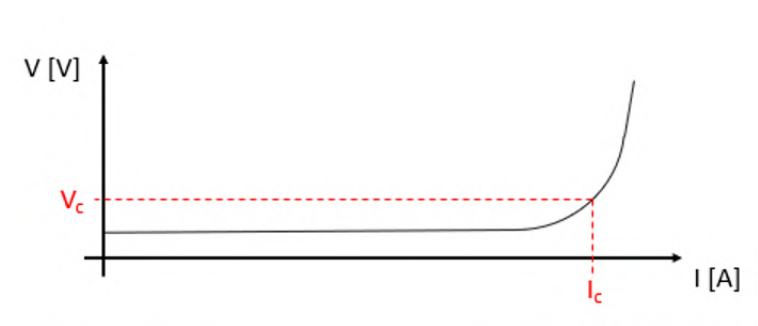


Figure 1: Typical current-voltage characteristic of an HTS device

According to Ohm's law ($V = RI$), the resistance corresponds to the slope of the IV characteristic.

The characterization of a short sample of HTS tape is standardized. The standard suggests that the IV characteristic be measured by the four-probe method. Its schematic is shown in Figure 2.

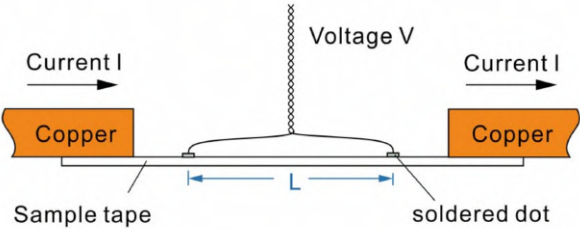


Figure 2: Schematic of the four-probe method

The current is supplied by a current source to two copper connectors in direct contact with the tape. Two potential taps are welded onto the tape 10 cm apart. The voltage between the 2 taps is measured by a nano-voltmeter as the current is increased in small steps. The curve obtained is the IV characteristic of the HTS tape.

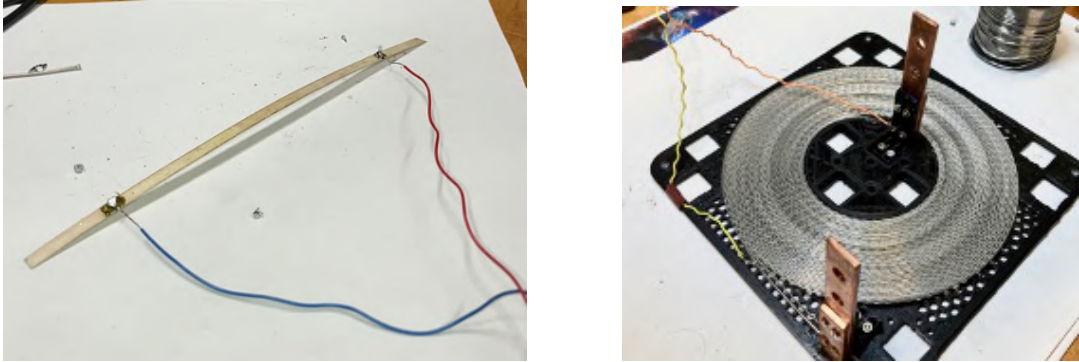


Figure 3: HTS tape and HTS coil

HTS tapes are wound into HTS coils to be used in HTS devices, Fig. 3. When adapting the standard to HTS coils, numerous problems are given when welding the potential taps onto the coil. Therefore, a new methodology is proposed: measuring the potential difference directly from the copper connectors of the support, as pictured in Figure 4.

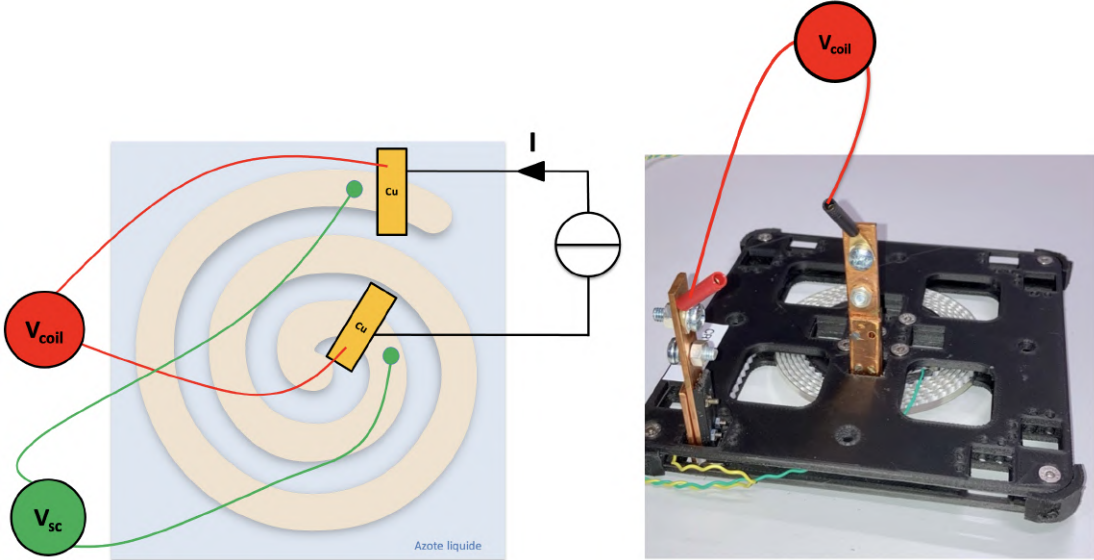


Figure 4: Proposed measurement protocol

Our efforts are focused on the computation of the additional resistance that appears

on the IV characteristic measured, to remove it in order to obtain the actual IV characteristic of the HTS coil.

We measure both V_{coil} and V_{sc} on the coil to compare them and draw conclusions about the nature of the resistance of the connectors. We call V_{conn} the voltage difference in each copper connector, obtaining the following equation:

$$V_{sc} = V_{coil} - 2 \cdot V_{conn} \quad (1)$$

where $V_{conn} = R_{conn} \cdot I$ and R_{conn} is the resistance of a single copper connector. By identifying R_{conn} , we will be able to estimate V_{sc} from V_{coil} .

Results

In Figures 5 and 6, we can see the IV characteristic of each coil measured using the two methods.

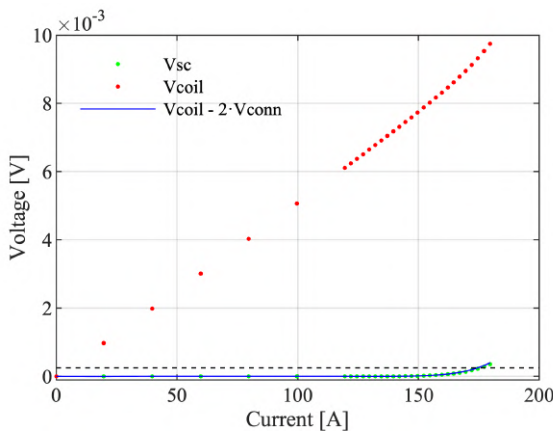


Figure 5: Measure on the 2.5m inductive coil and second order fit

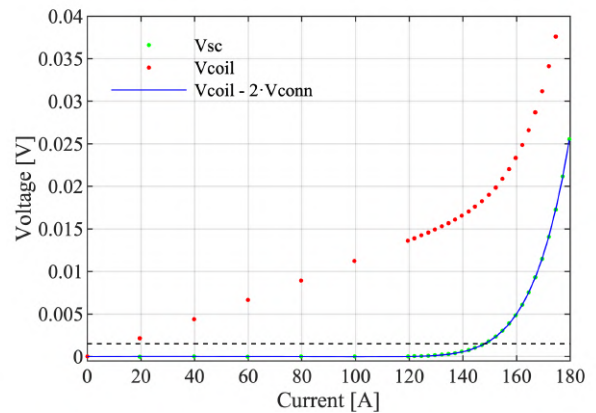


Figure 6: Measure on the 15m inductive coil and second order fit

To identify the connector voltage, a post-processing is done assuming that the connector voltage is of 2nd order.

$$V_{conn} = R_c I + R_d I^2 \quad (2)$$

The results of the post-processing shown in Figure 5 and 6 show that we can estimate the superconductor voltage V_{sc} from the measure of V_{coil} .

To discuss the assumption on the connector voltage order, we made a 3D finite element thermoelectric simulation of the connector. When the results obtained for V_{conn} by the simulation are compared to the ones obtained experimentally, a clear difference is

visible. This indicates that the numerical model must continue to be improved. In an attempt to understand the cause of this discrepancy, we carried out a sensitivity analysis. However, this numerical simulation allowed us to confirm that the resistance is in fact a not constant function of the current.

Conclusions

By post processing the measurements made in the laboratory and by making a numerical simulation of the copper connector, we were able to determine that its resistance is not constant. This resistance is best approximated as a linear function of the current, corresponding to a second order voltage drop. We are now able to remove the connectors' effect from the IV characteristic.

The proposed measurement technique is from our point of view an improvement on the conventional technique, since it removes the difficulty of welding the potential taps on the HTS material. A simple characterization technique is of interest to speed up the adoption of HTS devices.



Grado en Ingeniería en Tecnologías Industriales

Trabajo de Fin de Grado

Characterization of HTS Coils

Autor: Celia Gómez Limia

Director: Loïc Quéval

Madrid
Junio 2022

Abstract

The main objective of this project is to contribute to the standardization of the measurement of the current-voltage (IV) characteristic of superconducting coils. To this end, several experiments have been performed with superconducting tapes and coils. A new way to perform the characterization of HTS coils, without welding potential taps on the superconducting material, is proposed. Its accuracy is verified by comparing the obtained IV characteristic with the one obtained using the conventional method. The discussion is completed with a finite element simulation of the connector.

Keywords: high-temperature superconductor, IV characteristic, HTS tape, HTS coil, critical current

Acknowledgements

I would like to thank, first of all, my parents for giving me the opportunity to come to study in France at CentraleSupélec and for always supporting me unconditionally. Second but not least, my deepest thanks go to my project supervisor, Loïc Quéval, for constantly helping me throughout the year despite some difficulties and for introducing me to the interesting world of superconductivity.

Contents

1	Introduction	1
2	State of the art	3
2.1	IV characteristics of an HTS device	3
2.2	IV characteristics of an HTS tape	4
2.3	IV characteristics of an HTS coil	4
3	Project definition	7
3.1	Motivation	7
3.2	Objectives	7
3.3	Resources	8
3.4	Alignment with Sustainable Development Goals	9
4	Measure of the IV characteristic of HTS tapes	10
4.1	Experimental setup	10
4.2	Results	12
4.3	Summary	13
5	Measure of the IV characteristic of HTS coils	14
5.1	Problems encountered	14
5.1.1	Length, Inductivity	15
5.1.2	Welding of the potential taps	16
5.2	Measurements	18
5.2.1	Experimental setup	18
5.2.2	Results	18
5.2.3	Post-processing	19
5.3	Numerical simulation	21
5.3.1	Materials' properties	22
5.3.2	Physics modules	23
5.3.3	Results for a fixed current	26
5.3.4	Results for a sweep on the current	27
5.4	Comparison	30
5.4.1	Sensitivity analysis	31
5.5	Summary	31

CONTENTS

v

6 Conclusion

34

Bibliography

35

List of Figures

1.1	Superconducting Power Filter [3]	2
2.1	Typical current-voltage characteristic of an HTS device	3
2.2	Schematic of the four-probe method [12]	5
2.3	Distribution of the potential taps in the HTS coil [12]	5
3.1	HTS tape and HTS coil	8
3.2	Current source SORENSEN SGX 1200 DC.	9
3.3	Nano-voltmeter Keithley 2182A	9
4.1	HTS tape with its two potential taps	11
4.2	Cooling of the HTS tape	12
4.3	Electrical installation in liquid nitrogen	13
4.4	Measured IV characteristic of the HTS tape	13
5.1	Non-inductive coil	14
5.2	Inductive coil	15
5.3	Measured IV characteristics of a 15 m HTS inductive coil for 3 different time intervals: $\tau = 5, 10, 20$ s	16
5.4	Conventional measurement protocol	17
5.5	Proposed measurement protocol	18
5.6	2.5m inductive coil	19
5.7	15m inductive coil	19
5.8	Measure on the 2.5m inductive coil	19
5.9	Measure on the 15m inductive coil	19
5.10	Post-processing Matlab 15m coil - Hypothesis: Constant resistance	20
5.11	Post-processing Matlab 15m coil - Hypothesis: Linear resistance	21
5.12	Post-processing Matlab 2.5m - Hypothesis: Linear resistance	21
5.13	Connector and its 3D model	22
5.14	Electrical resistivity ρ copper R=100	23
5.15	Thermal conductivity k copper R=100	23
5.16	Heat capacity ($d \cdot c_p$) copper R=100	24
5.17	Terminal 1 and Terminal 2	25
5.18	Electric potential - 3D volume plot	26

5.19	Current density - 3D surface plot	26
5.20	Temperature - 3D surface plot	26
5.21	Electrical conductivity - 3D slice plot	26
5.22	Terminal's voltage as a function of the current	27
5.23	Total resistance as a function of the current	27
5.24	Comparison between fits for the 2.5m coil	28
5.25	Comparison between fits for the 15m coil	29
5.26	Comparison of voltage difference across the connector computed with the measures from the lab and by the numerical simulation	30
5.27	Comparison of the results obtained by the simulation when varying the value of RRR	31
5.28	Comparison of the results obtained by the simulation when varying the value of T_{ext}	32
5.29	Comparison of the results obtained by the simulation when varying the value of h_{tc}	32

List of Tables

4.1	Orders of magnitude	10
5.1	Stainless steel's properties	22
5.2	Comparison parameters R_{conn} obtained by the numerical simulation and in the laboratory	30

Chapter 1

Introduction

A growing number of everyday processes are being decarbonized, such as transportation or home conditioning. This transition generates an increased need for electricity, which means that we will need to transport more and more electricity.

In this context, where electricity transmission plays a key role, we are interested in making it as efficient as possible, reducing losses and increasing the volume transported.

Conventional power transmission lines are composed of resistive conductors, generally made of aluminum or copper. In these lines we witness Joule losses due to the resistance that the material opposes to the passage of current, causing part of the energy to be dissipated in the form of heat. In Spain, losses in the transmission of electricity at high voltage vary between 1% and 2% and, in the distribution phase, at medium and low voltage, between 6% and 8% of the electricity is lost [1]. These losses have both economical and environmental negative effects, as part of the energy produced is wasted.

Under these circumstances, the development of superconductivity in the power sector is of interest.

Among other properties, a superconductor has zero resistivity when cooled down below its critical temperature. A superconducting power cable can therefore carry high currents with negligible losses.

However, the conditions under which a material becomes superconducting are not easily achieved. As of today, practical materials must be operated at cryogenic temperature. This is why, since the discovery of superconductivity, much research has been done and many milestones have been achieved but it is still a work in progress.

Other superconducting devices have been proposed to operate in the power grids [2]. Among others, the "superconducting power filter" aims to increase the stability of DC grids by adding a current dependent resistance to the power line [3, 4, 5, 6]. A superconducting power filter is built using a non-inductive HTS coil.

To be able to use such device, we need to characterize it. The first step is to characterize the HTS coil. There is no standard to measure the characteristic of an HTS coil. This is therefore the focus of this project.

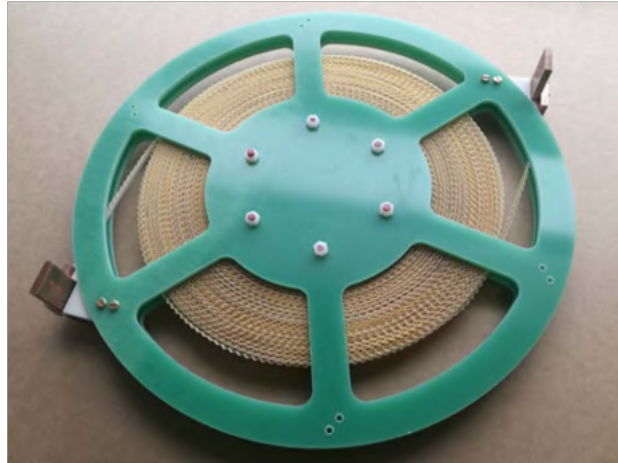


Figure 1.1: Superconducting Power Filter [3]

Chapter 2

State of the art

2.1 IV characteristics of an HTS device

The current-voltage (IV) characteristic of an HTS device is the graph representing the steady-state voltage of the HTS device as a function its current. The typical IV characteristics of an HTS device is illustrated in Figure 2.1.

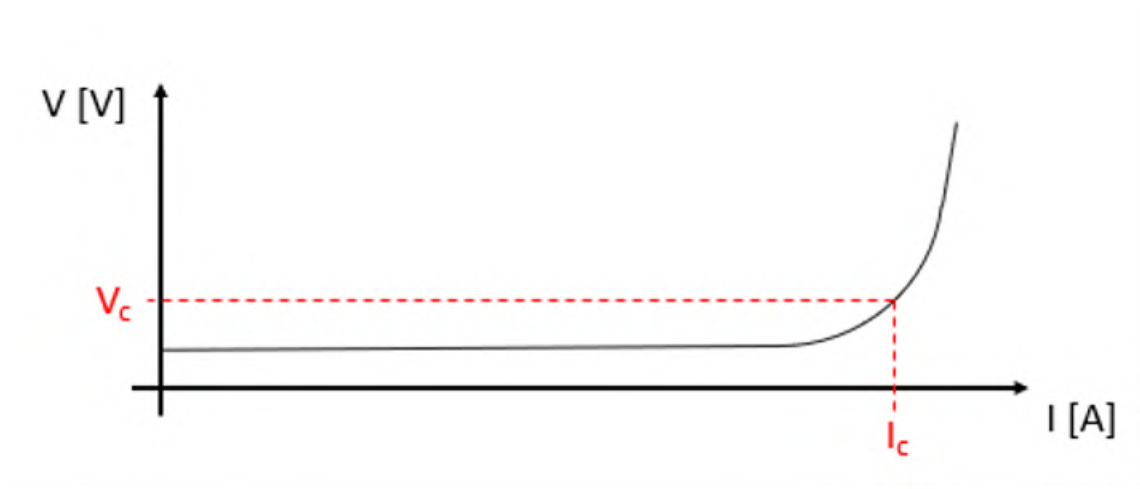


Figure 2.1: Typical current-voltage characteristic of an HTS device

According to Ohm's law ($V = RI$), so the resistance corresponds to the slope of the IV characteristic.

The IV characteristic can be generally well fitted by the power law,

$$V = V_c \left(\frac{I}{I_c} \right)^n \quad (2.1)$$

where V is the voltage of the device, I is the current of the device, V_c is the critical voltage and I_c is the critical current. n is the power law index.

The critical voltage V_c is obtained by multiplying a voltage criterion E_c , expressed in $\mu\text{V}/\text{m}$, by the HTS tape length L_{sc} ,

$$V_c = E_c \cdot L_{sc} \quad (2.2)$$

The critical current is the value of the current for which the device voltage is equal to the critical voltage. It is a parameter of the device that defines its current-carrying capacity [7, 8]. As a first approximation, one can say that: under the critical current the device is superconducting, while above the critical current the device is resistive. Above the critical current, a non-negligible quantity of energy is dissipated by Joule effect, there is a risk of thermal run away and of damaging the material.

The power law index n is a parameter of the device that defines the shape of the transition between its superconducting and its resistive state.

2.2 IV characteristics of an HTS tape

The measure of the critical current is standardized for HTS tapes [9]. We summarize here several key aspects of this standard.

The critical current is obtained from the IV characteristic of the HTS tape measured by to the four-probe method. Its schematic is shown in Figure 2.2. Note that the four-probe method is widely used to measure the critical current of both HTS tapes and coils [10], [11].

The current is supplied by a current source to two copper connectors in direct contact with the tape. The current is measured by an ammeter.

Two potential taps are welded onto the tape. They must be 10 cm apart. The voltage between the 2 taps is measured by a nano-voltmeter.

For HTS tapes, the voltage criterion is set to $E_c = 100\mu\text{V}/\text{m}$. Therefore, for the standard measure, the critical current is obtained when the HTS tape voltage is equal to 10 μV .

Note that several other criteria could have been used to define the critical current of a tape [13], but this discussion was settled by the standard.

2.3 IV characteristics of an HTS coil

HTS tapes are wound into HTS coils to be used in HTS devices. The measure of the critical current is not yet standardized for HTS coils.

Some researchers proposed to use the same voltage criteria of 100 $\mu\text{V}/\text{m}$ for HTS coils as for HTS tapes [14], [15].

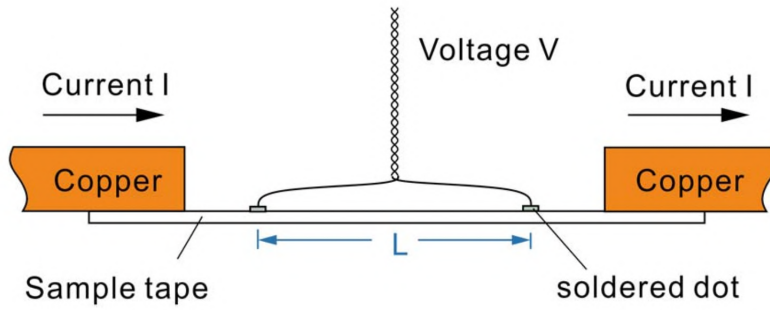


Figure 2.2: Schematic of the four-probe method [12]

A study was done by a group from the School of Electrical Engineering and Automation, Harbin Institute of Technology, in 2016 to determine the critical current of an HTS coil measuring the IV characteristic between different parts of the coil [12]. Seven pairs of potential taps were welded at different parts of the coil, which are distributed to the straight-line segment and bending segment in the innermost, middle and outermost turns of the HTS coil, as shown in Figure 2.3.

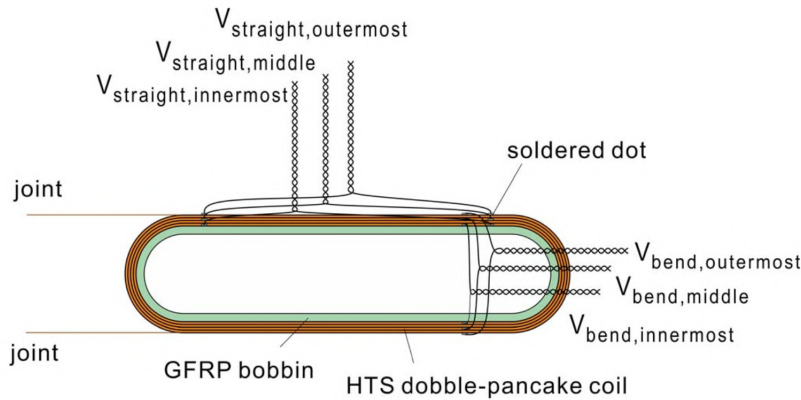


Figure 2.3: Distribution of the potential taps in the HTS coil [12]

The IV characteristic is measured for each pair of voltage taps (following the four-probe method) and the critical current is calculated (along with n) with curve fitting. Different results were obtained for each pair of voltage taps, leading to different values of I_c , some below the I_c calculated of the total coil.

The authors of that study suggested to embed the voltage taps in the innermost turn of

the HTS coil in order to measure the critical current of the HTS coil, if possible, as its voltage will rise earlier most of the time. The IV characteristic of the straight segment of the HTS coil's innermost and outermost turn should be both measured and used as the criteria to calculate the critical current. The smaller critical current can be defined as the critical current of the HTS coil.

Researchers in Cambridge, U.K., built a model in 2012 of high-temperature superconducting pancake coils using the finite element method to calculate current and magnetic field distribution inside the coil [16]. They found that $100 \mu\text{V}/\text{m}$ was too high a criterion to determine long-term operating current of the coils, because the innermost turns of a coil will, due to the effect of local magnetic field, reach their critical current much earlier than outer turns. Their modeling showed that an average voltage criterion of $20 \mu\text{V}/\text{m}$ over the coil corresponds to the point at which the innermost turn electric field exceeds $100 \mu\text{V}/\text{m}$. So $20 \mu\text{V}/\text{m}$ is suggested to be the voltage criterion of the HTS coil.

Chapter 3

Project definition

3.1 Motivation

The motivation of this project is to contribute to the characterization of HTS coils. The measure of the IV characteristic of a short length HTS sample is standardized. But the measure of the IV characteristic of an HTS coil is not yet standardized.

A new method for measuring the IV characteristic of HTS coils is proposed in order to avoid welding the potential taps on the superconducting material.

The adoption of this characterisation technique by the standardisation committee would facilitate the use of superconducting coils and speed up the implementation of superconductivity in the electric grid.

3.2 Objectives

The first objective was to become familiar with the manipulations on superconducting materials at the laboratory and with the protocol. This objective was covered by measuring the IV characteristic of several superconducting tapes.

The second objective was to measure the IV characteristic of superconducting coils. The standard that already exists for measuring the IV characteristic of a superconducting tape had to be tested on a superconducting coil and adapted.

When working on this second objective, a third objective arose. The way to connect the voltage probe to the coil needed to be modified. A new technique was proposed, which had to be tested and verified.

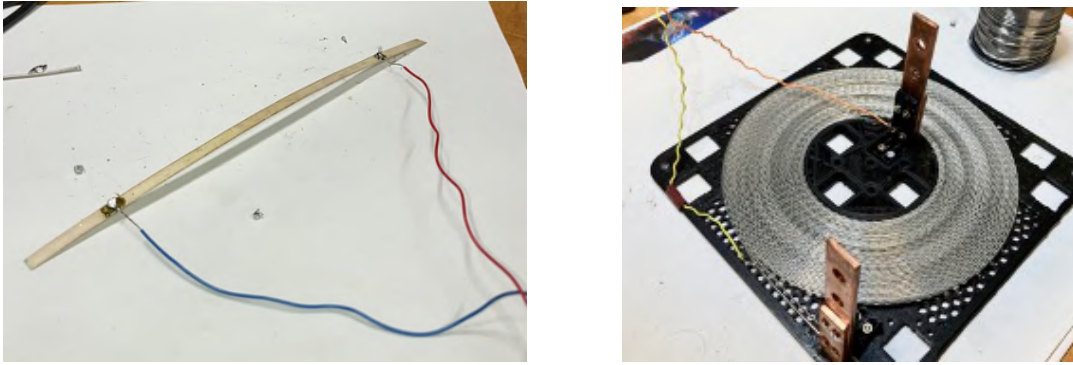


Figure 3.1: HTS tape and HTS coil

3.3 Resources

For the experimental work I have used resources provided by the GeePs laboratory, CentraleSupélec, University Paris-Saclay.

- European Standard IEC 61788-26:2020 [9]
- Liquid nitrogen (LN2)
- Support to insert the tape in the electric circuit that would be immersed in the polystyrene tray containing the liquid nitrogen.
- Current source SORENSEN SGX 1200 DC. (Figure 3.2)
- Nano-voltmeter Keithley 2182A (Figure 3.3)
- Matlab R2020b on Windows 10
- Personal protective equipment (gloves, goggles)

For the measures on HTS tapes, I used BSCCO tapes.

For the measures on HTS coils, I used 2 coils that were wound as part of the PhD thesis of Rafael Medeiros [17]. The first one is wound with 2.5 m of BSCCO on a support with copper connectors. The second one is wound with 15 m of BSCCO on a support with copper connectors.

We have also improved the existing Matlab code used to carry out the measurements. The postprocessing is made with Matlab as well.

For the numerical simulation of the copper connector I have used *Comsol Multiphysics* 6.0, provided by CentraleSupélec, on my personal computer. I have also used several tutorials provided by the software to develop our model.



Figure 3.2: Current source SORENSEN SGX 1200 DC.

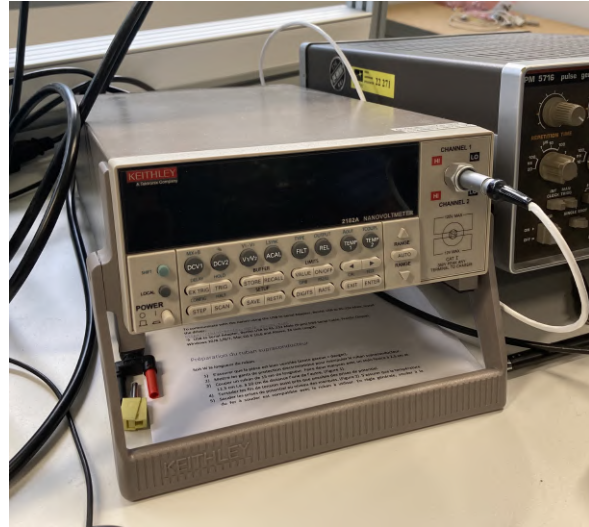


Figure 3.3: Nano-voltmeter Keithley 2182A

3.4 Alignment with Sustainable Development Goals

The Sustainable Development Goals are 17 goals to achieve a sustainable future for all. These goals incorporate the global challenges that society faces on a daily basis, such as poverty, inequality, environmental degradation, climate, peace, justice and prosperity. These goals are intended to be met by 2030.

We can relate this project to the following Sustainable Development Goals:

SDG 7: "Ensure access to affordable, reliable, sustainable and modern energy for all"

This project contributes to the development and standardization of superconducting devices for the electric grid. Such device could provide an economic and environmental improvement as the energy losses could be drastically reduced and the energy quality could be improved, thus enabling an affordable, reliable, sustainable and modern electric grid for all.

SDG 9: "Build resilient infrastructure, promote inclusive and sustainable industrialization, and foster innovation"

This project contributes to the development of superconducting technology, it can therefore be related, in particular, with the **Target 9.b:** "Support domestic technology development, research and innovation in developing countries, including by ensuring a conducive policy environment for, inter alia, industrial diversification and value addition to commodities".

Chapter 4

Measure of the IV characteristic of HTS tapes

In this chapter, we measure the IV characteristic of HTS tapes. The objective is to understand this measurement and to be able to perform it without difficulty.

For this stage of the project, I worked hand in hand with Marine HEYRAUD and Xavier CUNIN, both students at CentraleSupélec. We carried out the measurement of the IV characteristics of 10 HTS tapes.

In order to understand the difficulty of carrying such measurement, here are some orders of magnitude in Table 4.1: we need to measure a very small voltage by applying a very large current at a cryogenic temperature.

Parameter	Value
Voltage	10^{-6} V
Current	200 A
Temperature	77 K

Table 4.1: Orders of magnitude

4.1 Experimental setup

This measurement is standardized, that is to say that there is an established protocol for this measurement. This standardization allows to adjust the measurements made on the superconducting tapes to make them comparable. We have therefore followed the measurement of the standard to characterize the tapes. The protocol applied follows the European standard EN IEC 61788-26:2020 [9].

Following the standard, the superconducting tape must be at least 10 cm long, because the potential taps must be 10 cm apart. Therefore, we cut 15 cm of superconducting tape and welded the two potential taps to measure the voltage difference between them.

The potential is then recovered thanks to two small wires (in red and in blue on Figure 4.1) that will be connected to the nano-voltmeter in order to be able to measure the small voltage.

The difficulty here was to weld the wires to the superconducting tape since the taps are fragile. Sometimes, the tap came off from the tape during the measurements, which made us lose both time and money. We did not find any real solution to overcome this problem besides being extremely delicate during the handling of the HTS tape.

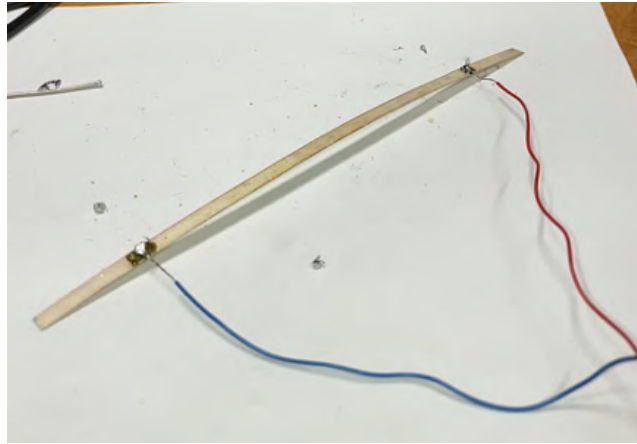


Figure 4.1: HTS tape with its two potential taps

The following step is to connect the HTS tape in series with the current source. To do so, we place the tape on a G10 support connected to the current source through two copper connectors which are in direct contact with the tape, as illustrated in Figure 4.2. These connectors are connected to the current source by the green and blue wires. In Figure 4.3, it is clearly visible that the wires carrying the current are thick because the current is large.

As mentioned earlier, the difficulty of working with superconducting material is that for them to work with superconducting properties, they need to be cooled down to cryogenic temperature. The liquid nitrogen helps us reach this temperature. The temperature of the bath reached about 77K, or -196°C . In Figure 4.3, we can see the process to cool down the sample: the support with the HTS tape is slowly submerged into a polystyrene tank filled with liquid nitrogen (LN2).

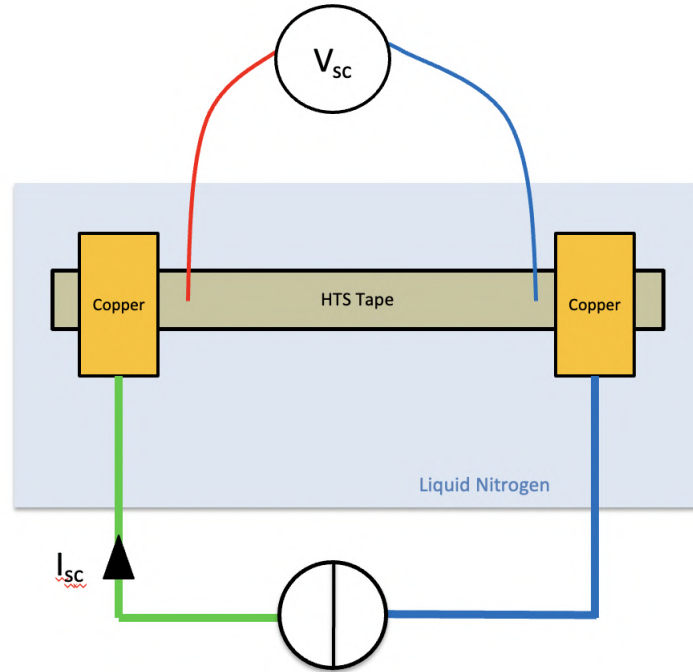


Figure 4.2: Cooling of the HTS tape

Once everything is connected, a Matlab script controls the current and the acquisition of the current and voltage. The current is increased in small steps according to the standard, the time interval between each measurement points was fixed at $\tau = 10s$.

4.2 Results

The measured IV characteristic of one of the HTS tapes is shown in Figure 4.4.

We observe that between 0 and 140A, the voltage is zero (the resistance is null). However, above 140A, the voltage increases little by little (the resistance increases). According to the standard, the critical current is defined for $V_c = 10\mu V$, as the distance between the potential taps is 10cm. By graphical reading, we deduce that the critical current is $I_c \approx 172A$. This is in agreement with the manufacturer datasheet (170 A).

This measure is fitted by the power law (Equation 2.1), in green in Figure 4.4. The results obtained are: $n = 16.83$ and $I_c = 171.68A$.



Figure 4.3: Electrical installation in liquid nitrogen

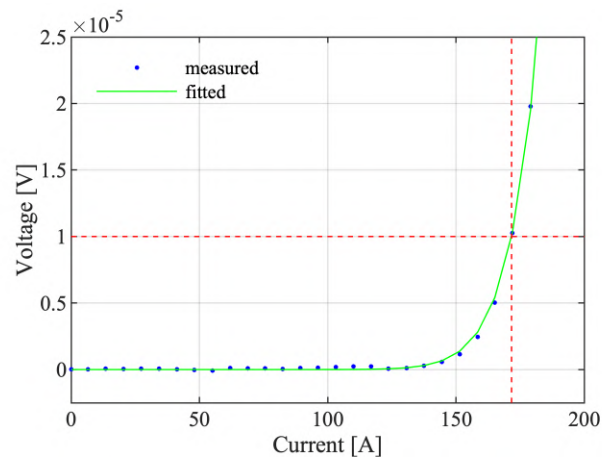


Figure 4.4: Measured IV characteristic of the HTS tape

4.3 Summary

In this section, we measured the IV characteristic of an HTS tape following the standard.

By doing so, we learned how to use the equipment of the lab and to carry out the measurement. The next step is to apply what we learned to measure the IV characteristic of an HTS coil.

Chapter 5

Measure of the IV characteristic of HTS coils

In this chapter, we measure the IV characteristic of HTS coils. The objective is to adapt the protocol used to characterize the HTS tapes to an HTS coil. Indeed, contrary to the measurement of the tape characteristic, the coil characteristic is not standardized. The goal is therefore to propose a standard for this measurement.

In this project, we will focus on the characterization of an inductive coil. The difference between a non-inductive and an inductive coil is the way in which the superconducting tape is rolled up, as we can appreciate in Figures 5.1 and 5.2.

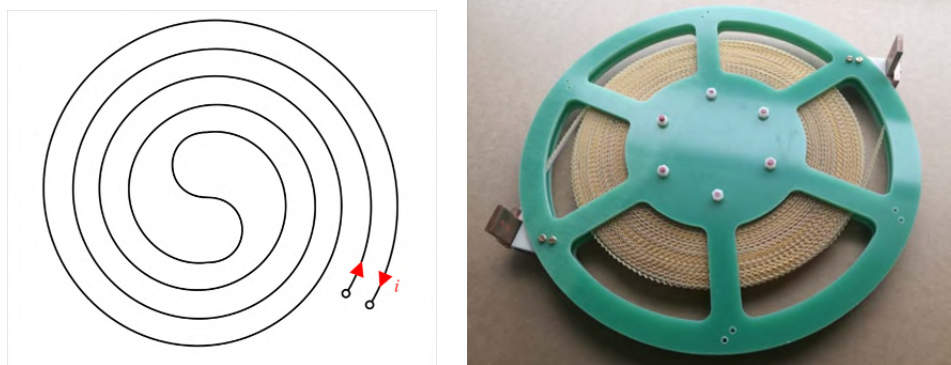


Figure 5.1: Non-inductive coil

5.1 Problems encountered

The measurement of the current-voltage characteristic of a superconducting coil poses several difficulties.

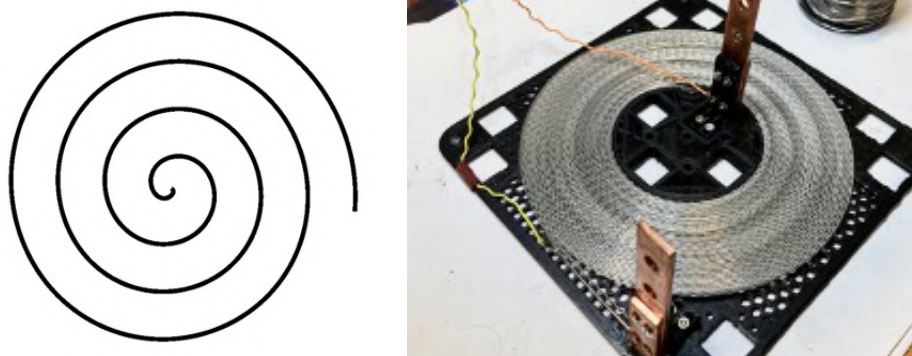


Figure 5.2: Inductive coil

First of all, in the case of an inductive superconducting coil, the inductance of the coil will cause a first difficulty: A coil has an inductance which is not negligible, contrary to that of a short superconducting tape.

Moreover, the coil is a tape wound on itself: thus, welding the potential taps at the ends of the coil can be complicated. Moreover, welding can damage the superconductor. A coil has a high economical cost, much more than a tape, and we can't afford to damage the coils. Welding is therefore a problem.

The challenge is to find a solution to measure the characteristic of a superconducting coil and to propose a valid protocol.

5.1.1 Length, Inductivity

A coil has an inductance, noted L , that we have to take into account during our measurements on it. Indeed, a term in $L \frac{di}{dt}$ will appear in the electrical equation: the current will present a transient regime which will be followed by a permanent regime.

It is therefore necessary to take into account during our measurements this transient regime characterized by a time constant that will depend on L . The more important L is, the bigger the time constant is and the longer the transient regime will be. Therefore, in theory, it would be necessary to wait longer between two measurements.

We sought to determine the optimal time interval τ between two measurement points: this corresponds to the minimum time interval that allows to take into account the transient regime mentioned above. This interval had been fixed at $\tau = 10s$ for the measurement on the superconducting tape.

A first test on a 15 m inductive coil was performed. The idea here was to test the measure for different τ in order to study the possible divergence between the results and thus adapt this time interval τ . This test was done using the same protocol that was used for the manipulations on HTS tapes, making a few adjustments to the Matlab code.

Three series of measurements were conducted for three different values of τ : 5 s, 10 s, 20 s.

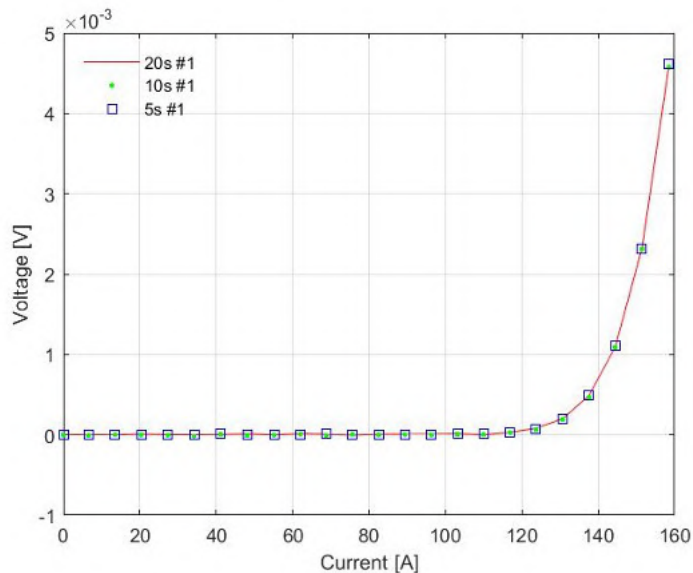


Figure 5.3: Measured IV characteristics of a 15 m HTS inductive coil for 3 different time intervals: $\tau = 5, 10, 20$ s

In Figure 5.3, we observe that the measurements are identical for these three time intervals tested. Thus, we deduce that for this coil, $\tau = 10$ s is suitable.

5.1.2 Welding of the potential taps

A second difficulty that we encountered was the welding of the potential taps on the coil.

The conventional measurement protocol, adapted from the one used for the HTS tape, is illustrated in Figure 5.4: the potential taps are welded at the beginning and at the end of the coil, i.e. in the center and the exterior of the spiral.

To avoid welding the potential taps onto the coil, we propose to measure the voltage directly on the copper connectors. The proposed measurement protocol is illustrated in Figure 5.5.

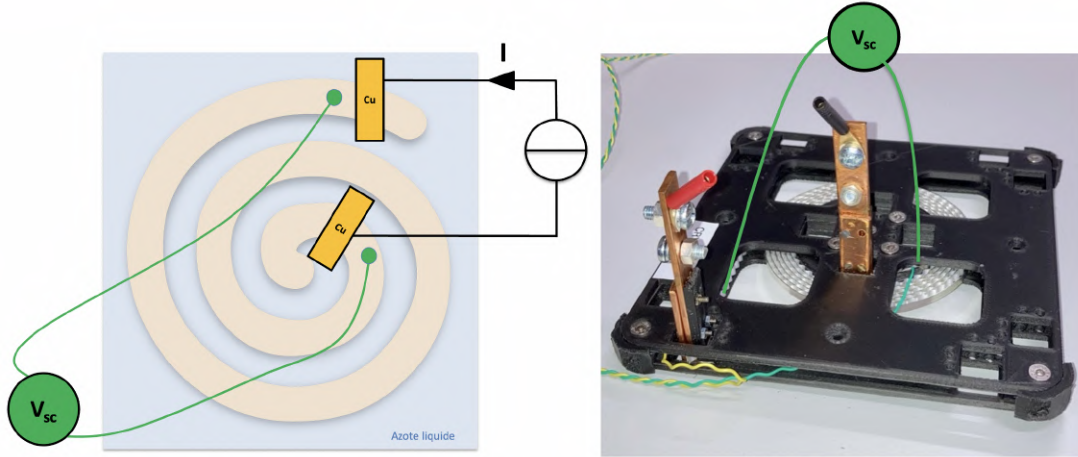


Figure 5.4: Conventional measurement protocol

With this proposed method, we can plot the IV characteristic of the HTS coil but there is an additional resistance that appears that corresponds to the copper connectors, and not just to the superconducting coil.

Our efforts are focused on the computation of this additional resistance, that appears on the IV characteristic measured, to remove it in order to obtain the actual IV characteristic of the HTS coil.

To do this, we will do the measure on the coil by the two different methods to compare them and draw conclusions about the nature of the resistance of the connectors. Following the notation on Figure 5.5, we will note V_{sc} the voltage measured by the conventional method, corresponding to the voltage difference in the superconductor, and V_{coil} the one measured by the proposed method. We will call V_{conn} the voltage difference in each copper connector, we will assume that its identical on both connectors. We obtain the following equation:

$$V_{sc} = V_{coil} - 2 \cdot V_{conn} \quad (5.1)$$

where $V_{conn} = R_{conn} \cdot I$ and R_{conn} is the resistance of a single copper connector. By identifying R_{conn} , we will be able to estimate V_{sc} from V_{coil} .

The steps to follow to determine the nature of this resistance and to verify the validity of the proposed method are:

1. Plot the I-V characteristic of an HTS coil according to each method. Post-processing the I-V characteristic obtained with the proposed method to remove the resistance associated to the connectors. This is done in section 5.2.

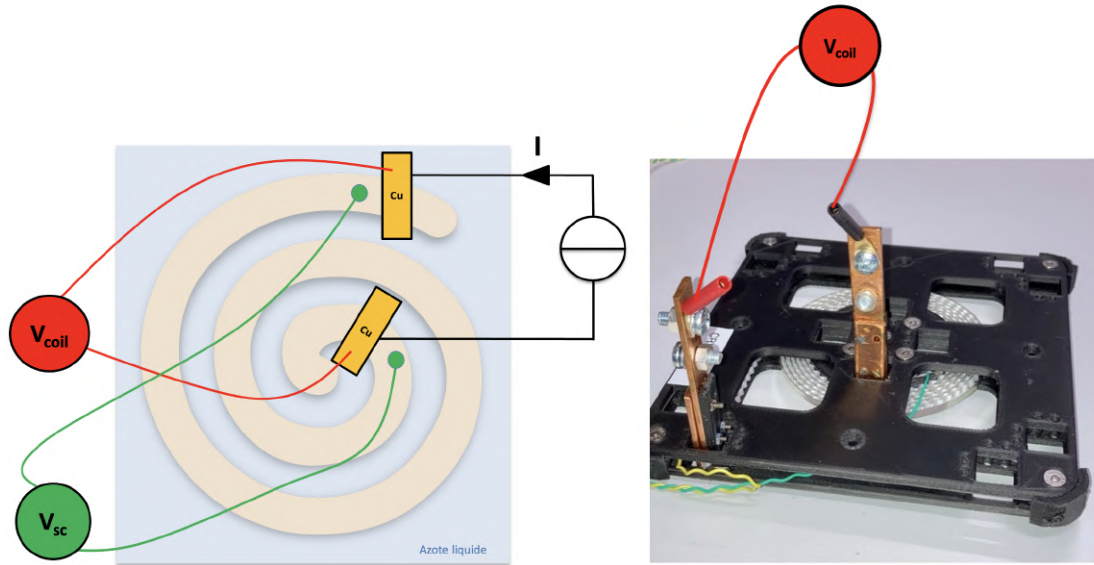


Figure 5.5: Proposed measurement protocol

2. Development a numerical simulation of the resistance of the copper connectors when passing current through them, and the corresponding voltage drop. This is done in section 5.3.
3. Comparison of the results obtained by the numerical simulation with the ones obtained experimentally. This is done in section 5.4.

5.2 Measurements

5.2.1 Experimental setup

The measures were done in the GeePs laboratory. Two different coils were used, one of 2.5 meters of HTS tape (Fig. 5.6) and another one of 15 meters (Fig. 5.7). Both coils are inductive. The same manipulation was done in both coils.

5.2.2 Results

In Figures 5.8 and 5.9, we can see the IV characteristic of each coil measured using the two methods.

There is a clear difference between both measures: on V_{coil} there is a resistance (slope) that appears from the start corresponding to the resistance of the copper connectors.

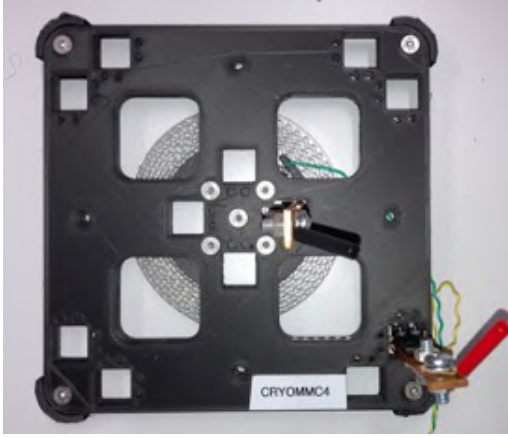


Figure 5.6: 2.5m inductive coil

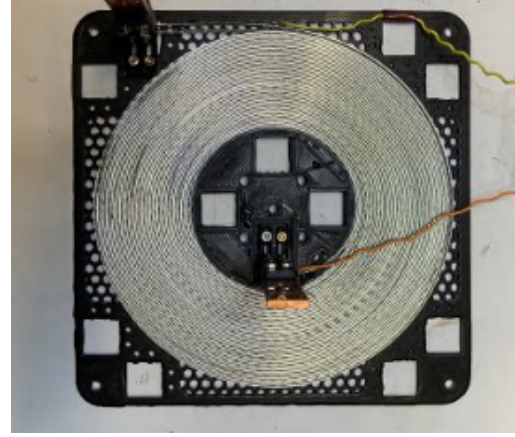


Figure 5.7: 15m inductive coil

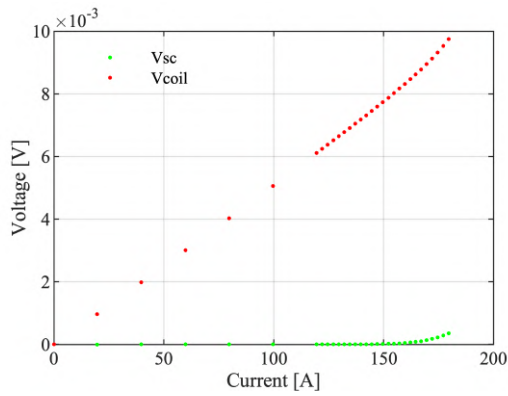


Figure 5.8: Measure on the 2.5m inductive coil

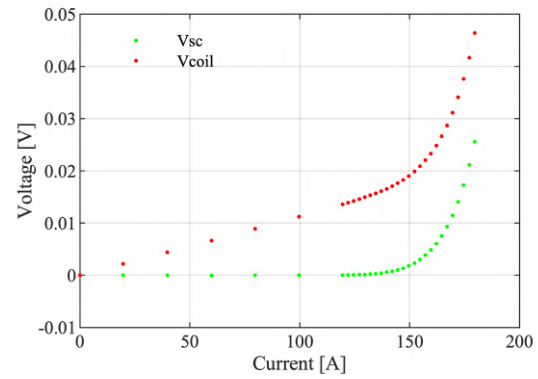


Figure 5.9: Measure on the 15m inductive coil

We want to be able to model this resistance to remove it from the data measured in order to get the IV characteristic corresponding only to the superconducting coil, V_{sc} . This will be done by numerical post-processing.

5.2.3 Post-processing

The objective is to find the relationship between both measurements, which will result on the resistance:

$$V_{sc} = V_{coil} - 2R_{conn}I \quad (5.2)$$

Our goal is therefore to approximate R_{conn} in order to remove the connectors effect on V_{coil} and get the closest possible to V_{sc} .

The post-processing was first done for the measures done on the 15m coil and later tested on the 2.5m coil.

First order

As a first step, we assume that the resistance is constant: $R_{conn} = R_c$. The corresponding voltage drop would be linear,

$$V_{conn} = R_c I \quad (5.3)$$

We calculated the slope of the linear part of V_{coil} , which would correspond to the resistance of both copper connectors ($2R_{conn}$), and multiplied by the current measured at each point. The value obtained was subtracted from all potential measurements of V_{coil} .

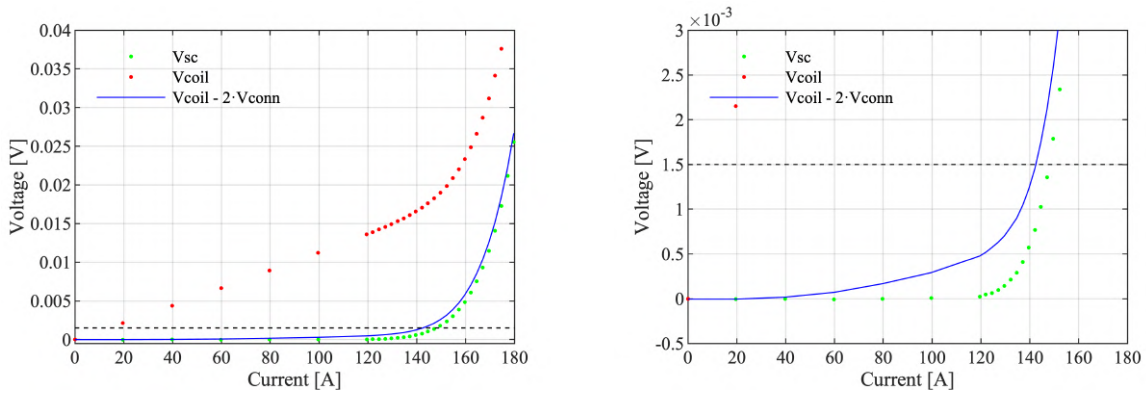


Figure 5.10: Post-processing Matlab 15m coil - Hypothesis: Constant resistance

We identified $R_c = -8.0624e - 09$. The results obtained are shown in Figure 5.10. When zooming in (picture on the right), we see $V_{coil} - 2 \cdot V_{conn} \neq V_{sc}$. There are clearly other effects to consider.

Second order

As a second step, we assume that the resistance is linear: $R_{conn} = R_c + R_d I$. The corresponding voltage drop would be of second order,

$$V_{conn} = R_c I + R_d I^2 \quad (5.4)$$

We identified $R_c = 5.4043e - 05$ and $R_d = 2.3720e - 08$. Graphically, we can see in Figure 5.11 that $V_{coil} - 2 \cdot V_{conn} \approx V_{sc}$. We seem to have found a pretty good approximation of the nature of the connector's resistance, corresponding to a second order voltage drop.

This fit was obtained using the measures done on the 15m coil. The results obtained when testing it on the 2.5m coil are shown in Figure 5.12, it seems to also work. For

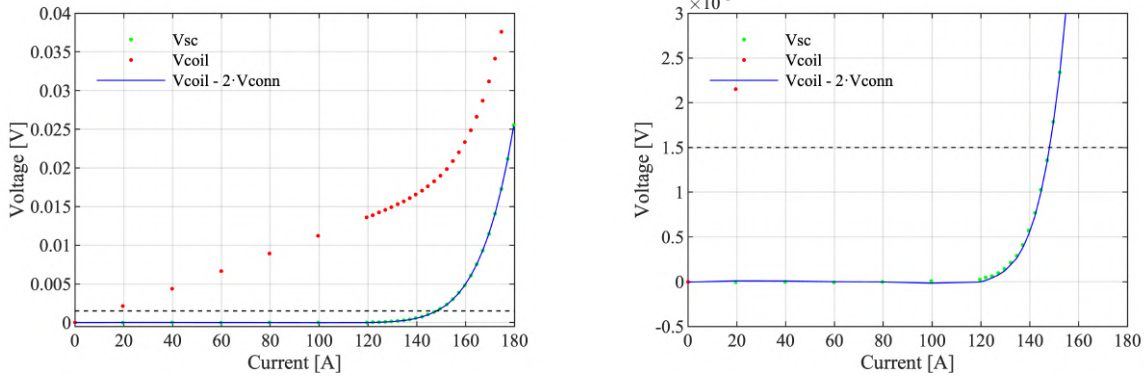


Figure 5.11: Post-processing Matlab 15m coil - Hypothesis: Linear resistance

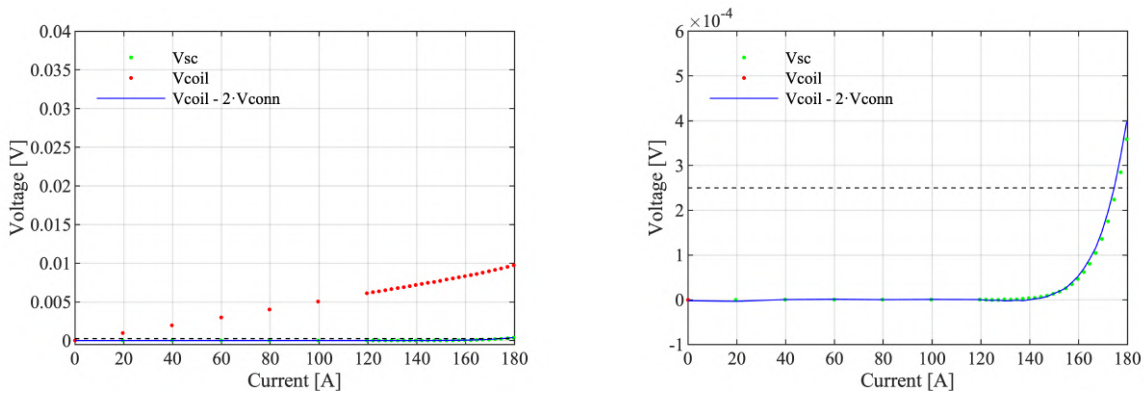


Figure 5.12: Post-processing Matlab 2.5m - Hypothesis: Linear resistance

the 2.5m coil we identified $R_c = 2.4660e - 05$ and $R_d = 7.5863e - 09$.

We now know how to model the influence of the connectors resistance. But there is a question that stays unanswered, why does it behave this way?

5.3 Numerical simulation

To understand why the connector creates a 2nd order voltage drop, we carried out a numerical simulation using the commercial software: "Comsol Multiphysics 6.0".

The objective is to model one of the connectors in 3D and compute its resistance and voltage drop when electric current passes through it. This results will be compared to the measurements.

We modelled the copper connector and a section of the superconducting tape that is in contact with the connector. As we are only looking at what happens in one connector, in our model the current will enter by one of the holes of the connector and it will exit

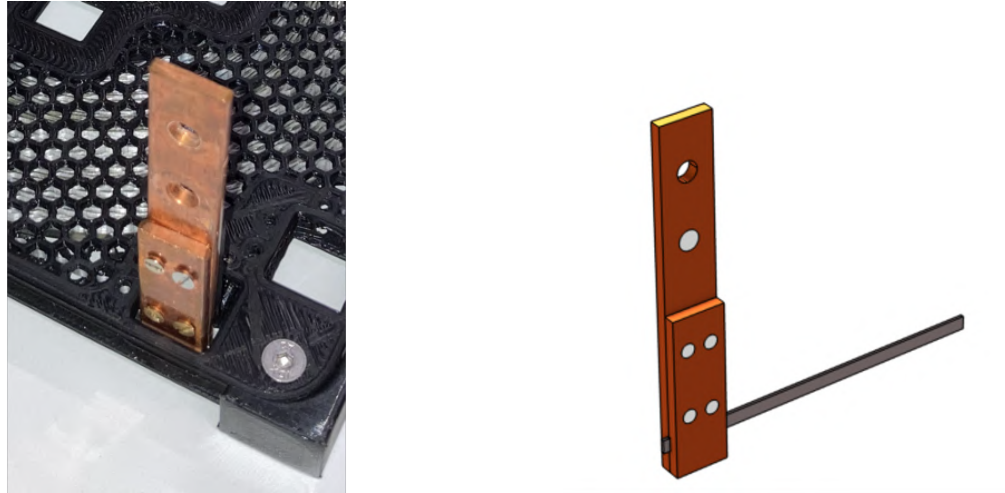


Figure 5.13: Connector and its 3D model

by the end of the tape.

The connectors used in the lab are not exactly the same, but they are very similar. For what follows, we have modeled one of the connectors used on the 15m coil.

Once we had drawn the geometry of the connector, we had to define the materials' properties and add the physics modules.

5.3.1 Materials' properties

For the superconducting tape, we created a new material that had a resistivity negligible in comparison to the copper resistivity. To assure this, we set its electrical conductivity to $\sigma = 10^{15}$ [S/m].

The connector's bolts have been modeled with stainless steel, whose properties can be found in Table 5.1.

Property	Value	Unit
Electrical conductivity	1.73913	MS/m
Relative permittivity	1	
Thermal conductivity	15	W/(m·K)
Density	7.93 e3	kg/m ³
Heat capacity	502	J/(kg·K)

Table 5.1: Stainless steel's properties

The copper connector has been modeled with a material with copper's properties at cryogenic temperatures described by the National Institute of Standards and Technology [18] [19], for standard copper we set the residual resistance ratio to $RRR = 100$.

- Electrical resistivity ρ [$\Omega \cdot \text{m}$] traced in Figure 5.14
- Thermal conductivity k [$\text{W}/(\text{K} \cdot \text{m})$] traced in Figure 5.15
- Volumetric heat capacity, which is equal to its mass density $d = 8960$ [kg/m^3] multiplied by its specific heat c_p [$\text{J}/(\text{K} \cdot \text{kg})$], traced in Figure 5.16

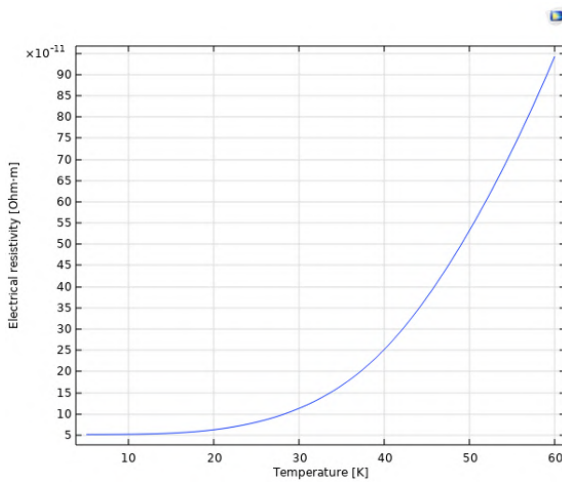


Figure 5.14: Electrical resistivity ρ copper R=100

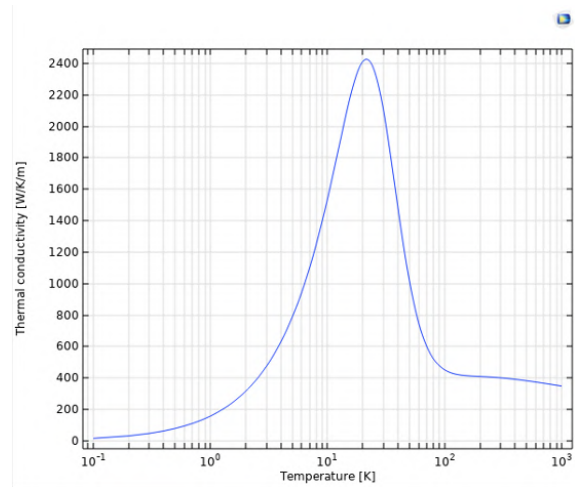


Figure 5.15: Thermal conductivity k copper R=100

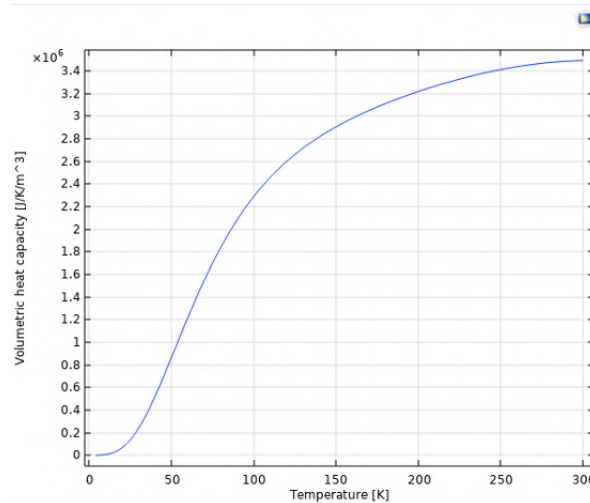
5.3.2 Physics modules

Once the geometry of the connector has been drawn and the materials have been defined, the physics must be added. For our simulation, we will make use of the "electric currents module" and the "heat transfer module", both of which will have to be coupled.

Electric currents

In this module, the following variables will be used:

- J [A/m^2] Current density
- Q [C] Charge


 Figure 5.16: Heat capacity ($d \cdot c_p$) copper R=100

- σ [S/m] Electrical conductivity
- E [V/m] Electric Field
- V [V] Electric potential

This module implements the current conservation equation, Ohm's law and the equation relating the gradient of the electric potential to the electric field:

$$\nabla \cdot J = Q_{J,V}$$

$$J = \sigma E + J_e$$

$$E = -\nabla V$$

Electric insulation is defined on all boundaries, $n \cdot J = 0$, except for the two terminals that are defined: Terminal 1, the surface through which a current I_0 enters, and Terminal 2, the surface that is set to the ground voltage, where the current exits our model. These terminals are pictured in Figure 5.17

Heat transfer

In this module, the following variables will be used:

- ρ [kg/m³] Volumetric density
- C_p [J/(K·kg)] Heat capacity
- u [m/s] Speed

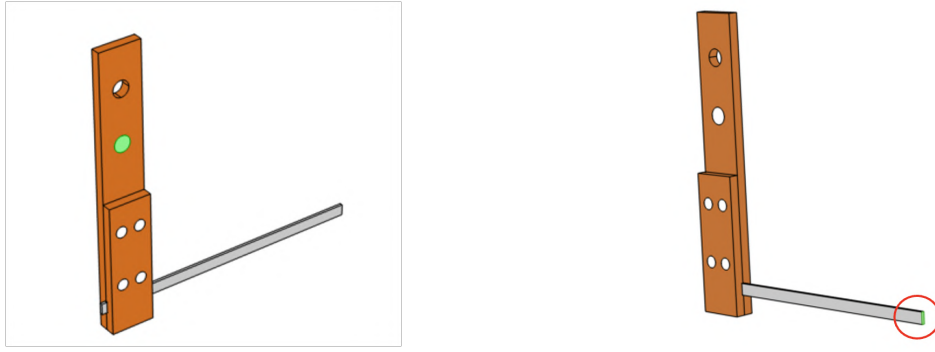


Figure 5.17: Terminal 1 and Terminal 2

- T [K] Temperature
- q [W/m²] Heat flux
- Q [W] Heat transfer
- k [W/(K·m)] Thermal conductivity
- h [W/(K·m²)] Heat transfer coefficient

This model applies the energy heat balance and Fourier's law:

$$\rho C_p u \cdot \nabla T + \nabla q = Q + Q_{ted}$$

$$q = -k \nabla T$$

Heat flux is defined as the exchange with the outside environment which, in our case, is the liquid nitrogen.

$$-n \cdot q = q_0$$

$$q_0 = h(T_{ext} - T)$$

The terminals are thermally insulated: $-n \cdot q = q_0$

Coupling interfaces

Both interfaces are coupled by adding a new variable in the heat balance equation to refer to the Joule effects:

$$\rho C_p u \cdot \nabla T = \nabla \cdot (k \nabla T) + Q_e$$

$$Q_e = J \cdot E$$

5.3.3 Results for a fixed current

The first simulation was done for a fixed current, to see if the simulation had physical sense. We set the current to 120 A and we got the results shown in Figures 5.18 5.19, 5.20 and 5.21.

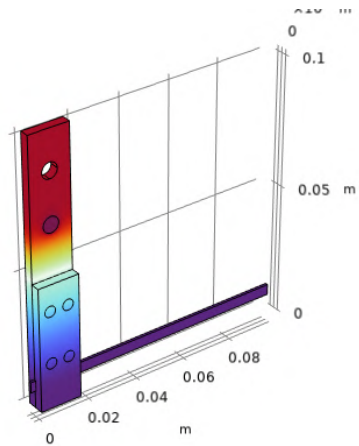


Figure 5.18: Electric potential - 3D volume plot

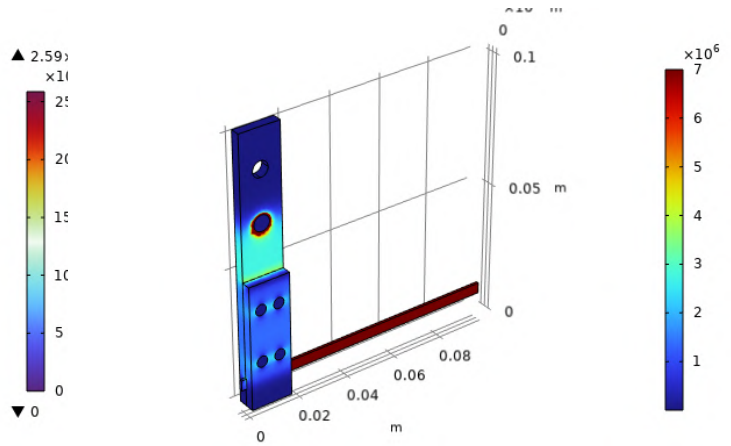


Figure 5.19: Current density - 3D surface plot

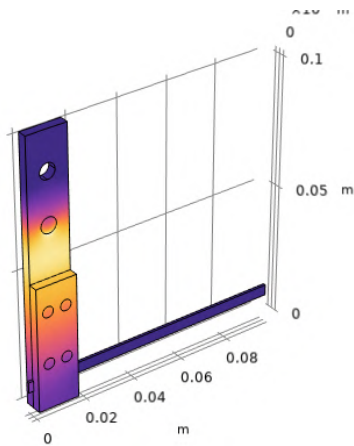


Figure 5.20: Temperature - 3D surface plot

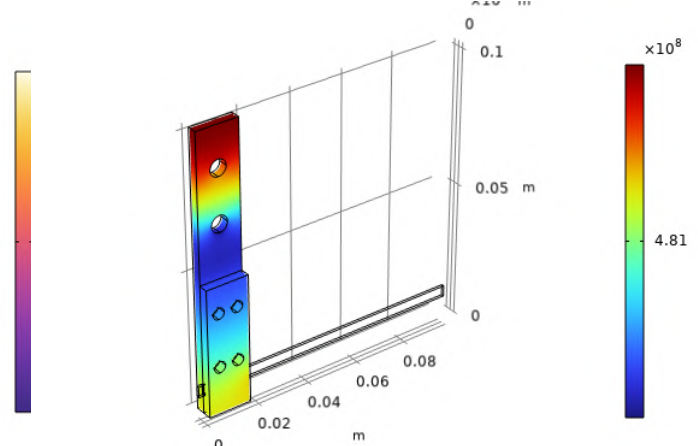


Figure 5.21: Electrical conductivity - 3D slice plot

From these results, we can deduce that the simulation has physical sense. The electric potential (Fig. 5.18) gradually descends towards the low of the figure, which corresponds to the fall in potential that we expected to see, V_{conn} , and the potential in the superconducting tape is constant, due to its high conductivity. Above the terminal where the current enters the figure, the potential is constant, as there is no current

going through this section, as it is visible in Fig. 5.19. In this last figure, we can see that the current goes down the connector and through the HTS tape, in this last one with a much higher current density, due to the high electric conductivity of the superconductor. In Fig. 5.20, we see that the copper heats up where the current density is higher, this corresponds to the Joule effects. Finally, as defined in the copper's properties, the resistivity will increase with temperature, i.e. the conductivity will decrease with temperature, this is visible in Fig. 5.21, as it is analogue to Fig. 5.20.

5.3.4 Results for a sweep on the current

To get the connector voltage and resistance as a function of the current, we do a parametric sweep on the current: $I = \{20, 40, 60, 80, 100, 120, 140, 160, 180\}$.

The terminal voltage V_{conn} , which corresponds to the voltage difference across the connector is plotted in Figure 5.22. The software is also able to compute the resistance of the connector R_{conn} , which is plotted as a function of the current in Figure 5.23.

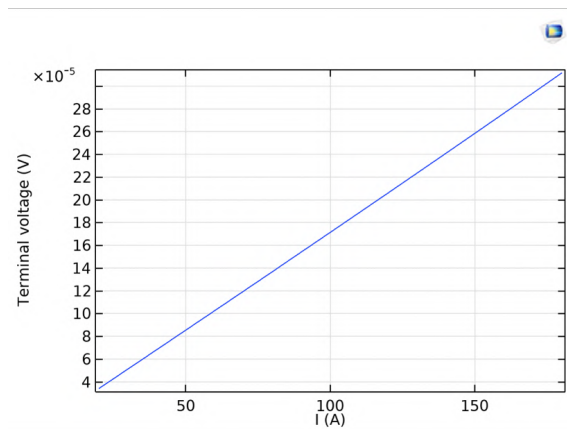


Figure 5.22: Terminal's voltage as a function of the current

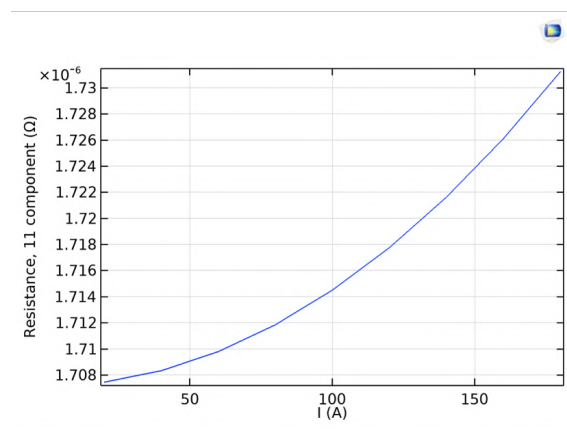


Figure 5.23: Total resistance as a function of the current

From these results, in Figure 5.23, we can see that the connector's resistance would be best fitted with at least a second order function of current, which would correspond to a third order voltage drop. However in section 5.2 the hypothesis of a second order voltage drop was made.

To compare these hypothesis, given by the results of the numerical simulation and by the post-processing of the measurements from the lab, we will compare the four different fits proposed in this paper. The first order voltage drop was the first guess made in section 5.2 that was proofed to not be very effective, the second order voltage drop was the best fit found in said section. Following the results obtained by the numerical simulation, we are going to test two new fits: a third and fourth order voltage drop.

This comparison is shown in Figure 5.24, for the 2.5m coil, and in Figure 5.25 for the 15m coil. We computed $2 \cdot V_{conn}$ for each fit to then remove it from the V_{coil} measured. This value is compared with the V_{sc} measured by calculating the error between both values.

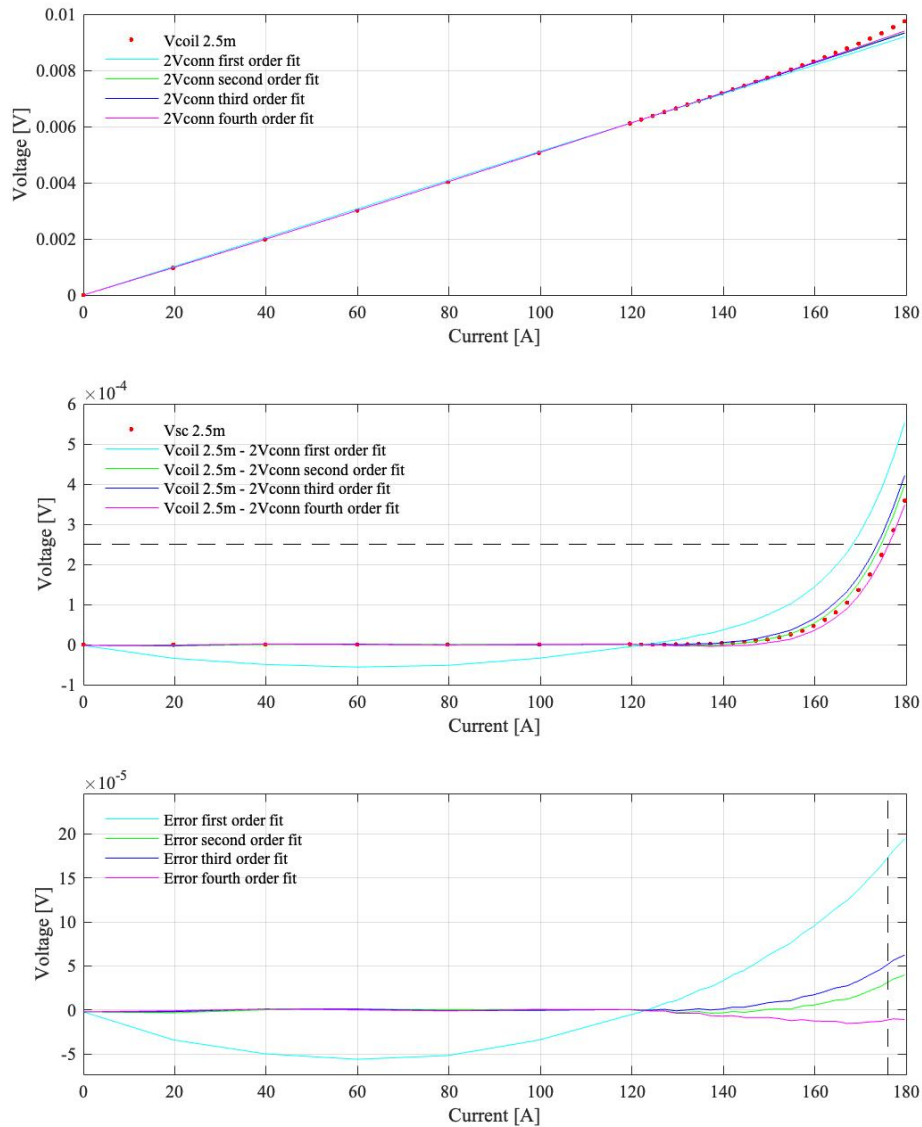


Figure 5.24: Comparison between fits for the 2.5m coil

In Figures 5.24 and 5.25 we observe the results obtained for currents below the critical

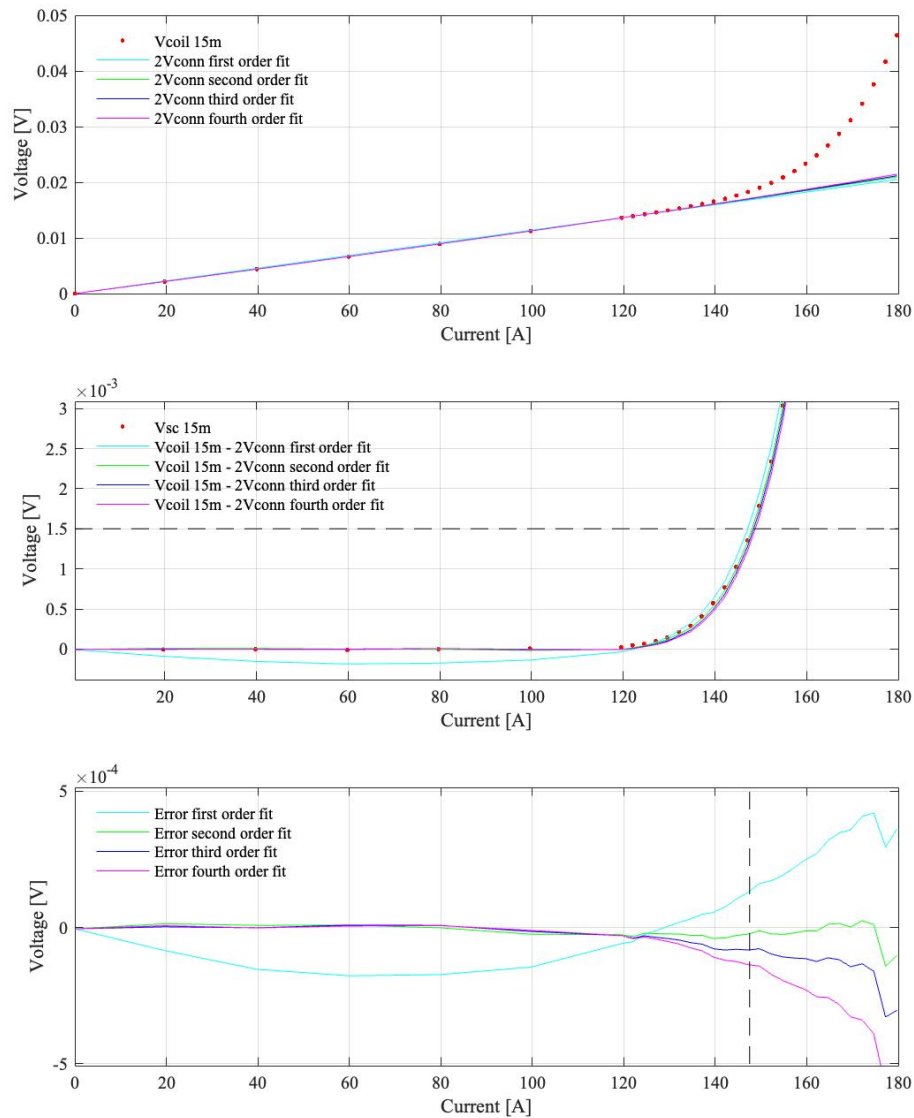


Figure 5.25: Comparison between fits for the 15m coil

current, which are the currents that interest us because above this current the coil is not considered superconducting.

We can see that for both coils, the worst fit is the first order fit, as expected. However, the best fit is not the same for both coils. For the 15m coil the most accurate fit is second order fit while for the 2.5m coil, it seems to be fourth order fit. Nevertheless,

the second order fit is a good trade-off between the results and the complexity.

5.4 Comparison

Finally, we compare the results obtained by the numerical simulation with the ones obtained by the post-processing of the measures done on the 15m coil in the lab. Following the results obtained in the previous section, we assume there is a second order voltage drop, and therefore, that the resistance is a linear function of the current:

$$V_{conn} = R_{conn} \cdot I$$

$$R_{conn} = R_c + R_d \cdot I$$

We group the results in Table 5.2 and graphically, in Figure 5.26.

	Lab	Simulation
R_c [Ω]	5.4043e-05	1.6964e-06
R_d [Ω]	2.3720e-08	1.8749e-10

Table 5.2: Comparison parameters R_{conn} obtained by the numerical simulation and in the laboratory

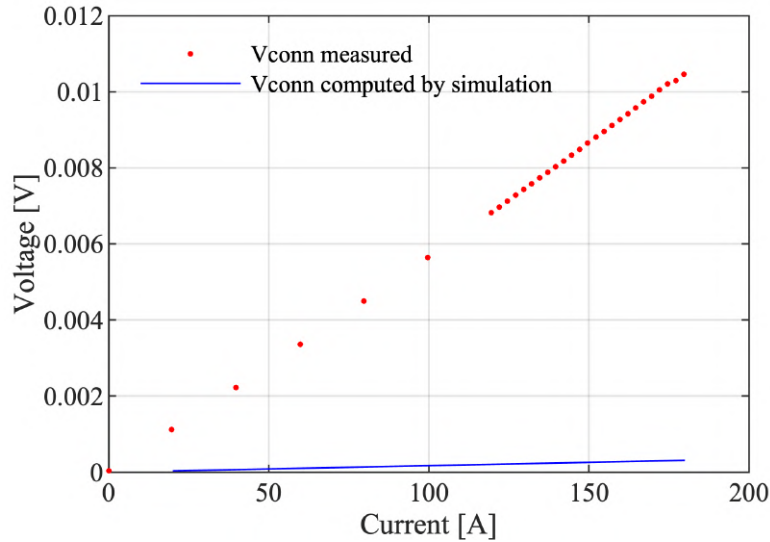


Figure 5.26: Comparison of voltage difference across the connector computed with the measures from the lab and by the numerical simulation

There is a clear difference between the results, which indicates that the numerical model must continue to be improved. In an attempt to understand the cause of this discrepancy, we carry out a sensitivity analysis in the following section.

5.4.1 Sensitivity analysis

We perform sensitivity analysis with 3 model parameters: The residual resistance ratio RRR , the temperature of the external environment in contact with the connector T_{ext} and the heat transfer coefficient between the external environment and the connector h_{tc} .

The RRR value for copper ranges between 5 and 5000 [20]. This parameter was initially set to $RRR = 100$, assuming that the copper was standard. We launched the simulation for different values of RRR , the results obtained for the connector voltage V_{conn} is illustrated on Figure 5.27.

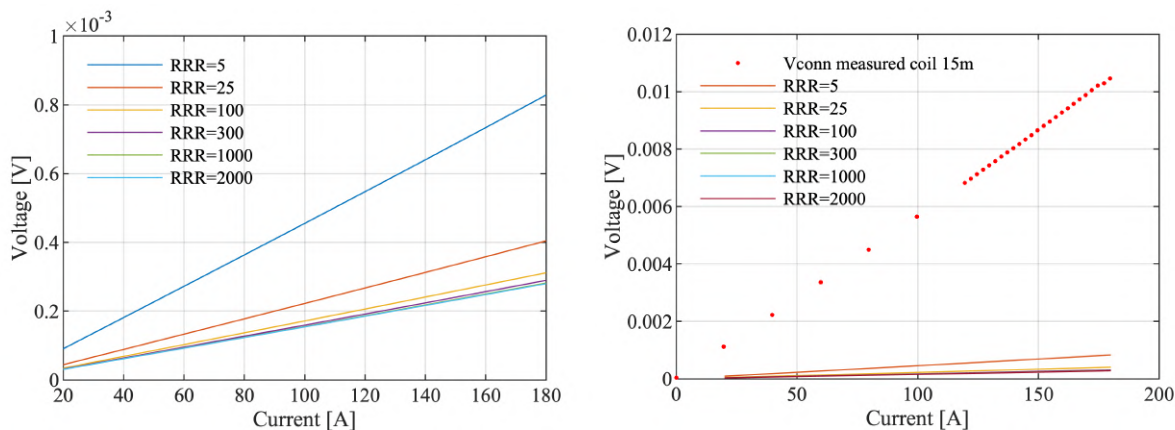


Figure 5.27: Comparison of the results obtained by the simulation when varying the value of RRR

The external temperature was initially fixed to 77K, as it corresponds to the temperature of the liquid nitrogen, which surrounds the connectors. However, there are bubbles that appear during the manipulations because of the heating of the copper. This leads us to believe that the temperature may not be exactly 77K... We tested running the simulation for different values of T_{ext} and saw the impact on the the voltage difference across the connector V_{conn} , the results are illustrated on Figure 5.28.

The heat transfer coefficient between the copper and the liquid nitrogen surrounding it, was initially set to $h_{tc} = 25 \text{ W}/(\text{K}\cdot\text{m}^2)$. This value is approximated, we check then to see the impact on the simulations result when varying it, this is pictured on Figure 5.29.

5.5 Summary

In this chapter, we have evaluated the two problems that we had encountered when adapting the protocol established for HTS tapes to HTS coils.

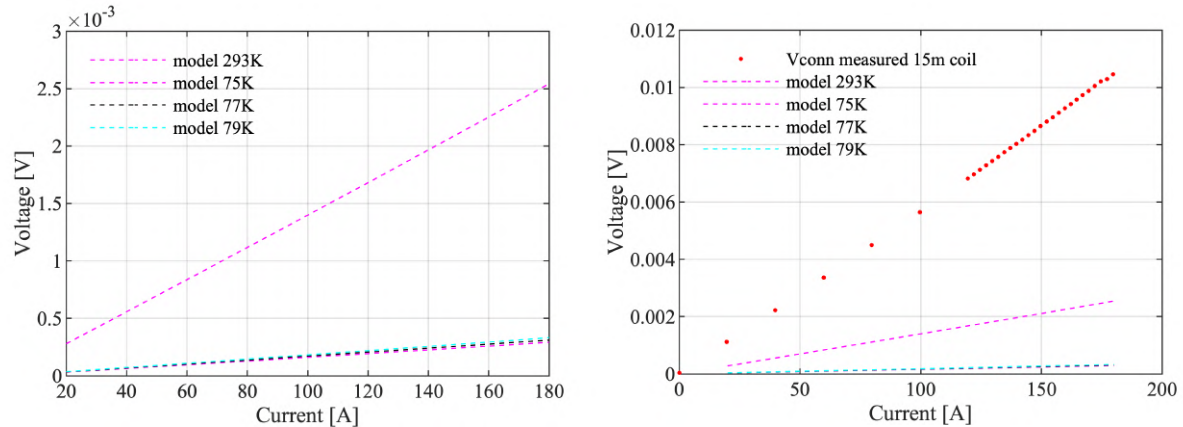


Figure 5.28: Comparison of the results obtained by the simulation when varying the value of T_{ext}

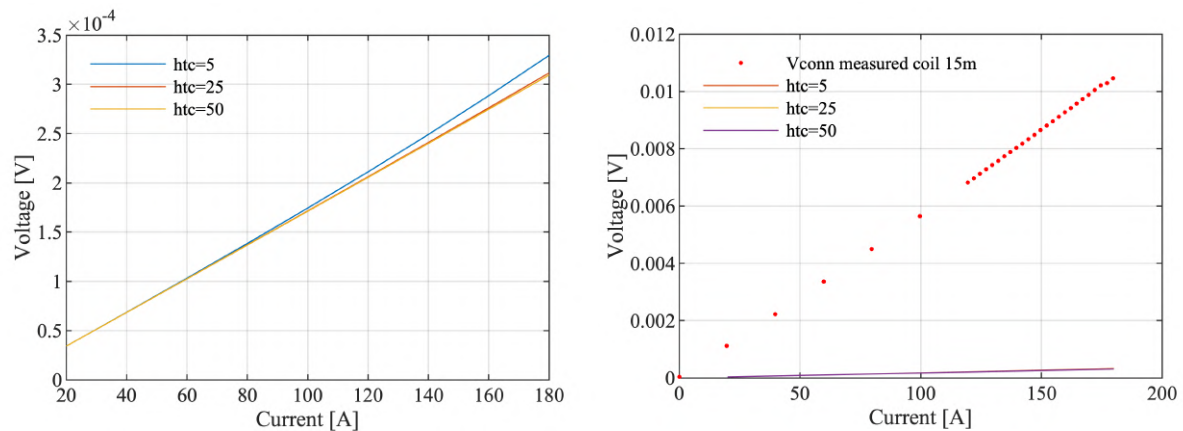


Figure 5.29: Comparison of the results obtained by the simulation when varying the value of h_{tc}

Firstly, we have seen that, for these coils, the time interval between two measurements does not directly affect the result, contrary to what was expected because of the inductance of the coil. We have therefore not changed this value value in relation to the manipulations performed on the tape.

Secondly, to avoid welding the potential taps on the coil, which causes numerous difficulties, we introduce another technique. This technique consists in measuring the potential difference directly on the copper connectors of the support.

To obtain the superconductor voltage from the coil voltage, the connector voltage has to be identified. This is done by post-processing assuming that the connector voltage is of 2nd order. The results show that we can estimate the superconductor voltage from the measures.

To discuss the assumption on the connector voltage order, we made a 3D finite element thermoelectric simulation of the connector. These results are compared and commented.

A sensitivity analysis is done to understand the parameters that have the most influence on the results and to understand the disparity between the numerical results and the experimental results.

Chapter 6

Conclusion

This work focuses on the adaptation of the standardized measurement of the current-voltage characteristic of an HTS tape to an HTS coil.

First, the characterization of HTS tapes was explained and tested, following the standard. Later on, when testing this measurement on HTS coils, we encountered numerous problems with the welding of the potential taps onto the superconducting material, so a new measurement method was proposed.

The proposed method consisted of measuring the potential difference from the copper connectors that are in direct contact with the ends of the HTS coil. The measured characteristic corresponded to the sum of the characteristic of the HTS coil and of the copper connectors. In this work we have calculated the value of the connectors' resistance in two different ways: by post processing the measurements made in the laboratory and by making a numerical simulation of the copper connector. Thanks to both we were able to determine that this resistance is not constant. It is best approximated as a linear function of the current, corresponding to a second order voltage drop. We are now able to remove the connectors' effect from the IV characteristic.

The proposed measurement technique is from our point of view an improvement on the conventional technique, since it removes the difficulty of welding the potential taps on the HTS material. A simple characterization technique is of interest to speed up the adoption of HTS devices.

Bibliography

- [1] ABC. *Casi el 10% de la electricidad generada se pierde en transporte y distribuciones*. URL: https://www.abc.es/economia/abci-casi-10por-ciento-electricidad-generada-pierde-transporte-y-distribucion-200407120300-9622525689116_noticia.html. (accessed: 06.04.2022).
- [2] F. Z. Yi. “Plenary talk - Progress in production and performance of second generation (2G) HTS wires and practical applications”. In: *Proc. IEEE Int. Conf. ASEM D* Beijing, China, pp. 258–258 (2013).
- [3] B.Douine L.Quéval F.Trillaud S.Fawaz H.Menana I.Schwenker O.Despouys N.Ivanov. “Characterization of a superconducting power filter for embedded electrical grid application”. In: *IEEE Transactions on Applied Superconductivity* vol. 32, no. 4 (Jun. 2022).
- [4] F.Trillaud B.Douine L.Quéval. “Superconducting power filter for aircraft electric DC grids”. In: *IEEE Transactions on Applied Superconductivity* vol. 31, no. 5, pp. 1-5 (Aug. 2021).
- [5] L.Quéval O.Despouys F.Trillaud B.Douine. “Feasibility study of a superconducting power filter for HVDC grids”. In: *22nd European Conference on Power Electronics and Applications (EPE'20 ECCE Europe)* (Lyon, France, Sep. 2020).
- [6] L.Quéval F.Trillaud B.Douine. “DC grid stabilization using a resistive superconducting fault current limiter”. In: *International Conference on Components and Systems for DC grids (COSYS-DC 2017)* (Grenoble, France, Mar. 2017).
- [7] C. P. Bean. “Magnetization of high-field superconductors”. In: *Rev. Mod. Phys.* vol. 36, no. 1, pp. 31–39 (Jan.–Mar. 1964).
- [8] V.Lombardo E.Barzi D.Turrioni and A.V.Zlobin. “Critical currents of $YBa_2Cu_3O_{7-\delta}$ tapes and $Bi_2Sr_2CaCu_2O_x$ wires at different temperatures and magnetic fields”. In: *IEEE Trans. Appl. Supercond* vol. 21, no. 3, pp. 3247–3250 (Jun. 2011).
- [9] IEC 61788-26:2020. “Part 26: Critical current measurement - DC critical current of RE-Ba-Cu-O composite superconductors”. In: *TC 90 - Superconductivity* (2020).
- [10] Z. Zhang et al. “An experimental investigation of critical current and current distribution behavior of parallel placed HTS tapes”. In: *IEEE Trans. Appl. Supercond* vol. 25, no. 3, Art. ID 8000305 (Jun. 2015).

- [11] J.-H. Kim and S. Pamidi. “Electrical characteristics of 2G HTS tapes under DC current with AC ripple”. In: *IEEE Trans. Appl. Supercond* vol. 22, no. 3, Art. ID 5801104 (Jun. 2012).
- [12] Y.Jikun X.Fengyu C.Anbin L.Liyi H.Zhengnan C.Jiwei and C.Qingquan. “Study of Method of Measuring and Determining HTS Coil’s Critical Current With $V - I$ Properties Between Different Parts of the Coil”. In: *IEEE Trans. Appl. Supercond* vol. 26, no. 4 (Jun. 2016).
- [13] A.F.Clark and J.W.Ekin. “Defining critical current”. In: *IEEE Trans. Appl. Supercond* vol. 21, no. 3, pp. 3247–3250 (Jun. 2011).
- [14] J.Souc E.Pardo M.Vojenciak and F.Gomory. “Theoretical and experimental study of ac loss in high temperature superconductor single pancake coils”. In: *Supercond. Sci. Technol.* vol. 22, no. 1, Art. ID 015006 (Nov. 2009).
- [15] W. Yuan et al. “Theoretical and experimental studies on J_c and AC losses of 2G HTS coils”. In: *IEEE Trans. Appl. Supercond* vol. 21, no. 3, pp. 2441–2444 (Jun. 2011).
- [16] M. Zhang et al. “Study of second generation, high-temperature superconducting coils: Determination of critical current”. In: *J. Appl. Phys.* vol. 111, no. 8, Art. ID 083902 (Apr. 2012).
- [17] R. Coelho Medeiros. “Cryo-MMC : a modular multilevel converter with superconducting coupled arm coils”. In: (2022). PhD thesis, University Paris-Saclay, GeePs, Gif-sur-Yvette, France.
- [18] N.J.Simon E.S.Drexler and R.P.Reed. “Properties of Copper and Copper Alloys at Cryogenic Temperatures”. In: *NIST Monograph 177* (Feb. 1992).
- [19] Giulio Manfreda. “Review of ROXIE’s Material Properties Database for Quench Simulation”. In: *Magnets, Superconductors and Cryostats TE-MSD* EDMS Nr: 1178007 (Dec. 2011).
- [20] Patxi DUTHIL. “Materials properties at low temperature”. In: *CERN Accelerator School* (Erice,Sicilia - 2013). URL: https://indico.cern.ch/event/194284/contributions/1472798/attachments/281498/393574/CAS_propmat_2013.pdf.